

This is A Tribute To The Best TN of All Time

Hogan, Matthew¹ and Toki, Walter¹

February 19, 2019

¹ *Colorado State University, Fort Collins, USA*

Abstract

This is the abstract

Contents

1	Introduction	7
2	BANFF Likelihood	8
2.1	BANFF Treatment of ND Constraint	8
2.1.1	Constructing a Likelihood	9
2.1.2	BANFF Likelihood	10
2.1.3	Flux, Cross Section, and Detector Systematics	11
2.2	Usage of ND280 Psyche Software	14
3	PØD Selections and Data Samples	16
3.1	Global Reconstruction	16
3.2	Data Sets	17
3.3	PØD Selection Cuts	18
3.3.1	Pre-Selection Cuts	18
3.3.2	CC-Inclusive in FHC	20
3.3.3	CC-Inclusive in RHC	20
3.4	PØD Water-Out Samples	20
3.4.1	CC-Inclusive	21
3.4.2	CC-1 Track (CCQE Enhanced)	35
3.4.3	CC-N Tracks (CCnQE Enhanced)	35
3.5	PØD Water-In Samples	36
3.5.1	CC-Inclusive	36
3.5.2	CC-1 Track (CCQE Enhanced)	50
3.5.3	CC-N Tracks (CCnQE Enhanced)	50
3.5.4	Differences Between Water-Out and Water-In Samples	51

31	4 PØD-Only BANFF Parameterization	52
32	5 Fitter Validation	53
33	6 Fitter Results	54
34	7 Discussion	55
35	References	56
36	Nomenclature	57

List of Figures

2.1	BANFF ND280 NuMu and ANuMu Flux Binning Parameters	12
2.2	BANFF Pre-fit Flux Covariance Matrix	12
2.3	Cross Section Parameters Pre-fit Correlation Matrix	13
2.4	Fluxing Tuning Histogram for FHC Events	15
3.1	PØD Air FHC ν_μ CC-Inc. Lepton Cand. Reco. Momentum by True Particle	22
3.2	PØD Air FHC ν_μ CC-Inc. Lepton Cand. Reco. $\cos \theta$ by True Particle	23
3.3	PØD Air FHC ν_μ CC-Inc. Lepton Cand. Reco. Momentum by NEUT Mode	24
3.4	PØD Air FHC ν_μ CC-Inc. Lepton Cand. Reco. $\cos \theta$ by NEUT Mode	25
3.5	PØD Air FHC ν_μ CC-Inc. Lepton Cand. Reco. Momentum by True Topology	26
3.6	PØD Air FHC ν_μ CC-Inc. Lepton Cand. Reco. $\cos \theta$ by True Topology . . .	27
3.7	PØD Air FHC ν_μ CC-Inc. Lepton Cand. True E_ν by NEUT Mode	28
3.8	PØD Air RHC $\bar{\nu}_\mu$ CC-Inc. Lepton Cand. Reco. Momentum by True Particle	29
3.9	PØD Air RHC $\bar{\nu}_\mu$ CC-Inc. Lepton Cand. Reco. $\cos \theta$ by True Particle	30
3.10	PØD Air RHC $\bar{\nu}_\mu$ CC-Inc. Lepton Cand. Reco. Momentum by NEUT Mode	31
3.11	PØD Air RHC $\bar{\nu}_\mu$ CC-Inc. Lepton Cand. Reco. $\cos \theta$ by NEUT Mode	32
3.12	PØD Air RHC $\bar{\nu}_\mu$ CC-Inc. Lepton Cand. Reco. Momentum by True Topology	33
3.13	PØD Air RHC $\bar{\nu}_\mu$ CC-Inc. Lepton Cand. Reco. $\cos \theta$ by True Topology . . .	34
3.14	PØD Air FHC $\bar{\nu}_\mu$ CC-Inc. Lepton Cand. True E_ν by NEUT Mode	35
3.15	PØD Water FHC ν_μ CC-Inc. Lepton Cand. Reco. Momentum by True Particle	37
3.16	PØD Water FHC ν_μ CC-Inc. Lepton Cand. Reco. $\cos \theta$ by True Particle . .	38
3.17	PØD Water FHC ν_μ CC-Inc. Lepton Cand. Reco. Momentum by NEUT Mode	39
3.18	PØD Water FHC ν_μ CC-Inc. Lepton Cand. Reco. $\cos \theta$ by NEUT Mode . .	40
3.19	PØD Water FHC ν_μ CC-Inc. Lepton Cand. Reco. Momentum by True Topology	41
3.20	PØD Water FHC ν_μ CC-Inc. Lepton Cand. Reco. $\cos \theta$ by True Topology .	42

62	3.21 PØD Water FHC ν_μ CC-Inc. Lepton Cand. True E_ν by NEUT Mode	43
63	3.22 PØD Water RHC $\bar{\nu}_\mu$ CC-Inc. Lepton Cand. Reco. Momentum by True Particle	44
64	3.23 PØD Water RHC $\bar{\nu}_\mu$ CC-Inc. Lepton Cand. Reco. $\cos \theta$ by True Particle . .	45
65	3.24 PØD Water RHC $\bar{\nu}_\mu$ CC-Inc. Lepton Cand. Reco. Momentum by NEUT Mode	46
66	3.25 PØD Water RHC $\bar{\nu}_\mu$ CC-Inc. Lepton Cand. Reco. $\cos \theta$ by NEUT Mode . .	47
67	3.26 PØD Water RHC $\bar{\nu}_\mu$ CC-Inc. Lepton Cand. Reco. Momentum by True	
68	Topology	48
69	3.27 PØD Water RHC $\bar{\nu}_\mu$ CC-Inc. Lepton Cand. Reco. $\cos \theta$ by True Topology .	49
70	3.28 PØD Water FHC $\bar{\nu}_\mu$ CC-Inc. Lepton Cand. True E_ν by NEUT Mode	50

List of Tables

3.1	POT Used in This Analysis	17
3.2	PØD WT FV and Corridor Definition	20

1 Introduction

2 BANFF Likelihood

2.1 BANFF Treatment of ND Constraint

The primary goal of an oscillation experiment is to measure the parameters in a neutrino mixing matrix. All other parameters, while having some theoretical importance to fundamental physics, are nuisance parameters that must be accounted for. To understand the methodology of BANFF, it is relevant to understand the number of nuisance parameters that go into a ND+FD fit. The BANFF implementation aims to reduce the dimensionality, and hence complexity, of the problem by performing a separate analysis on the nuisance parameters that only the ND can measure. Then that information is propagated to the oscillation analysis for the FD data. Conceptually this approach has computational advantages and should provide the same result with a joint ND+FD analysis. However, information encoded in the ND measurements for shared nuisance parameters is inevitably lost in this “divide-and-conquer” approach.

The BANFF ND-only constraint between 2015 and 2018 is described in detail in T2K-TN-220[7]. While subsequent updates to the BANFF analysis increase the sample sizes and systematic parameterizations, the method has remained unchanged. It uses a frequentist approach to find the best nuisance parameter set to maximize a binned likelihood. The sets of nuisance, also called systematic, parameters in BANFF are

- cross section physics model parameters hereby denoted by \vec{x} ,
- neutrino flux binned in neutrino energy hereby denoted by \vec{b} , and
- detector systematics response weights that affect detector observables hereby denoted by \vec{d} .

A priori (prior) knowledge of \vec{x} and \vec{b} are available from external measurements and experiments. The \vec{d} parameters are penalty terms whose effect can be understood and mitigated

with control samples.

2.1.1 Constructing a Likelihood

We can define a binned likelihood for the ND280-only constraint with the nuisance parameters as

$$\mathcal{L}(\vec{x}, \vec{b} | \vec{N}_{\text{ND280}}^{\text{Data}}) = \mathcal{P}(\vec{x}, \vec{b}, \vec{d} | \vec{N}_{\text{ND280}}^{\text{Data}}) = \frac{\mathcal{P}(\vec{N}_{\text{ND280}}^{\text{Data}} | \vec{x}, \vec{b}, \vec{d})}{\mathcal{P}(\vec{N}_{\text{ND280}}^{\text{Data}})} \pi(\vec{x}) \pi(\vec{b}) \pi(\vec{d}), \quad (2.1)$$

where $\vec{N}_{\text{ND280}}^{\text{Data}}$ are the binned data measurements, $\pi(\vec{y} = \vec{x}, \vec{b}, \vec{d})$ are prior distributions which are assumed Gaussian distributions

$$\pi(\vec{y}) = \left(\frac{1}{(2\pi)^k \det(V_y)} \right)^{\frac{1}{2}} e^{\left(-\frac{1}{2} \Delta \vec{y} \cdot V_y^{-1} \cdot \Delta \vec{y}^T \right)}, \quad (2.2)$$

with V_y being the covariance matrix for \vec{y} and $\Delta \vec{y} = \vec{y} - \vec{y}_{\text{Nominal}}$ is the difference between the current and nominal set of vector parameters, and $\mathcal{P}(\vec{N}_{\text{ND280}}^{\text{Data}})$ is a normalization. We have used Bayes' theorem

$$\mathcal{P}(AB) = \mathcal{P}(B) \mathcal{P}(A|B) \quad (2.3)$$

to evaluate (2.1) as

$$\mathcal{P}\left(\underbrace{\vec{x}, \vec{b}, \vec{d}}_A \middle| \underbrace{\vec{N}_{\text{ND280}}^{\text{Data}}}_B\right) = \frac{\mathcal{P}(\vec{N}_{\text{ND280}}^{\text{Data}}, (\vec{x}, \vec{b}, \vec{d}))}{\mathcal{P}(\vec{N}_{\text{ND280}}^{\text{Data}})} \quad (2.4)$$

which we can further manipulate since the data are independent of the nuisance parameters

$$\mathcal{P}(\vec{N}_{\text{ND280}}^{\text{Data}}, (\vec{x}, \vec{b}, \vec{d})) = \mathcal{P}\left(\underbrace{(\vec{x}, \vec{b}, \vec{d})}_A, \underbrace{\vec{N}_{\text{ND280}}^{\text{Data}}}_B\right) = \pi(\vec{x}) \pi(\vec{b}) \pi(\vec{d}) \mathcal{P}(\vec{N}_{\text{ND280}}^{\text{Data}} | \vec{x}, \vec{b}, \vec{d}) \quad (2.5)$$

resulting in Equation (2.1). The assumption of a Gaussian prior in Equation (2.2) while not always truly Gaussian, allows for the use of a covariance matrix to describe the uncertainties and correlations in parameters. Once a maximum of the likelihood is found after marginalizing the effects of the systematics \vec{d} , the best fit values for \vec{b} and \vec{x} can be propagated to the oscillation analysis.

2.1.2 BANFF Likelihood

In practice maximizing the log-likelihood (LLH) is performed instead of maximizing the likelihood function. In addition, multiplying the LLH by -2 turns the maximization problem into a minimization one which programs like MINUIT are designed to find. To obtain the best set of parameters \vec{x} and \vec{b} from the ND280 data that minimize the $-2 \times \text{LLH}$, we need to predict how they affect our detector observables. Consider binned samples that select different charged current topologies. A convenient choice of observables for all the samples are the outgoing charged lepton l momentum P_l and angle $\cos \theta_l$ as measured in the ND since all the nuisance parameters affect these quantities. BANFF also uses an event-by-event weighting scheme to rapidly vary the event observables from detector systematics. With this treatment, the detector systematics \vec{d} are treated with a response \vec{r} and thus $P_l \rightarrow P_l(\vec{r})$ and $\cos \theta_l \rightarrow \cos \theta_l(\vec{r})$. We have the pieces needed to define the likelihood function used in ND-only BANFF analysis. For each $(P_l, \cos \theta_l)$ bin $i = 1, 2, \dots, M-1, M$, the likelihood for the ND-constraint is a ratio of the predicted events (\vec{N}^p) likelihood to the likelihood of the data events (\vec{N}^d)

$$\begin{aligned} \Lambda_{\text{ND280}}^r &= \frac{\mathcal{L}(\vec{N}^p(\vec{x}, \vec{b}, \vec{r}) | \vec{N}^d)}{\mathcal{L}(\vec{N}^d(\vec{x}, \vec{b}, \vec{r}) | \vec{N}^d)} \\ &= \left(\prod_{\vec{y}=\vec{x}, \vec{b}, \vec{r}} \frac{\pi(\vec{y})}{\pi(\vec{y}_{\text{Nom}})} \right) \left(\prod_{i=1}^M (\vec{N}_i^p)^{\vec{N}_i^d} \frac{e^{-\vec{N}_i^p}}{\vec{N}_i^d!} \right) \left(\prod_{j=1}^M (\vec{N}_j^d)^{\vec{N}_j^d} \frac{e^{-\vec{N}_j^d}}{\vec{N}_j^d!} \right)^{-1} \end{aligned} \quad (2.6)$$

where constant terms have been dropped for brevity. When taking $-2 \log$ of both sides, we use Wilks' theorem to define a chi-squared $\Delta\chi_{\text{ND280}}^2 = -2 \log \Lambda_{\text{ND280}}^r$ which is

$$\Delta\chi_{\text{ND280}}^2 = 2 \sum_{i=1}^M \left[\vec{N}_i^p(\vec{x}, \vec{b}, \vec{r}) - \vec{N}_i^d + \vec{N}_i^d \log \left(\frac{\vec{N}_i^d}{\vec{N}_i^p(\vec{x}, \vec{b}, \vec{r})} \right) \right] + \Delta\vec{x} \cdot V_x^{-1} \cdot (\Delta\vec{x})^T + \Delta\vec{b} \cdot V_b^{-1} \cdot (\Delta\vec{b})^T + \Delta\vec{r} \cdot V_r^{-1} \cdot (\Delta\vec{r})^T \quad (2.7)$$

where again constants were dropped from before. Since \vec{N}_i^p is a function the nuisance parameters, this is most generally written as

$$\vec{N}_i^p(\vec{x}, \vec{b}, \vec{r}) = \sum_{j=1}^{N_i^{\text{MC}}} \vec{b}_j(E_\nu) \times w_j^{\text{norm}} \times w_j^{\vec{x}}(\vec{x}) \times w_j^{\vec{d}}(\vec{r}) \times \delta_i(P_j(\vec{r}), \cos \theta_j(\vec{r}), s_j(\vec{r})) \quad (2.8)$$

where \vec{b}_j is the flux weight as a function of E_ν , w_j^{norm} is the POT normalization **Is this the POT weight? Originally denoted as xnorm in TN-166 which usually denotes cross section parameters**, $w_j^{\vec{x}}(\vec{x})$ is the weight function for the interaction cross section, $w_j^{\vec{d}}(\vec{r})$ is the detector systematics weights that are stored in the response functions \vec{r} , and $\delta_i(P_j(\vec{r}), \cos \theta_j(\vec{r}), s_j(\vec{r}))$ is like a Kronecker delta that indicates the correct observable bin if the event belongs in sample $s_j(\vec{r})$.

2.1.3 Flux, Cross Section, and Detector Systematics

The minimization of the LLH is attempted by exploring the multidimensional parameter space to as best as possible match the data and prediction. To understand the response of each systematic, a covariance matrix is built for each source. A combined covariance matrix is used in the BANFF analysis where each submatrix is initially uncorrelated with each other. The parameters in the covariance matrix are usually given a nominal value of one (1) unless a special value is needed with an uncertainty extracted using the Cholesky decomposition method. The development of each systematic uncertainty is briefly discussed

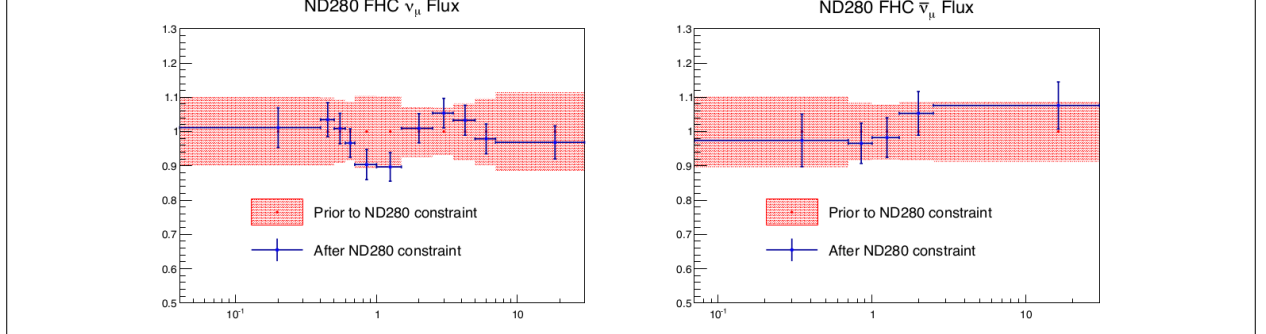


Figure 2.1: BANFF ND280 flux ν_μ and $\bar{\nu}_\mu$ binning parameters from T2K-TN-324 data post-fit results. The uncertainties are extracted from the pre-fit and post-fit covariance matrices.

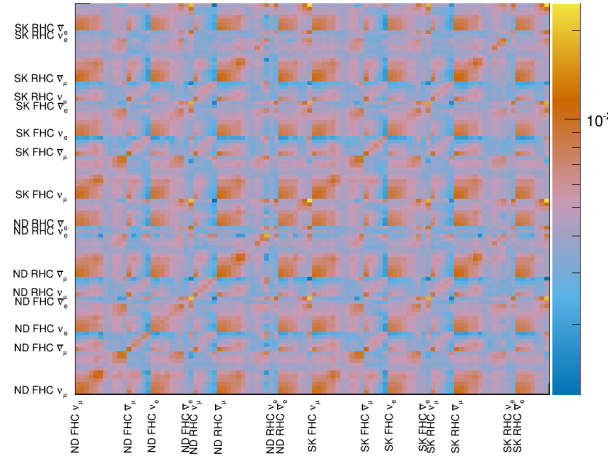


Figure 2.2: BANFF pre-fit flux covariance matrix shown with respective detector, horn current, and neutrino flavor.

below.

Flux: The flux weight is binned as a function of neutrino energy E_ν and divided by horn current (RHC or FHC) and neutrino flavor (ν_μ , $\bar{\nu}_\mu$, ν_e , and $\bar{\nu}_e$). Each flux bin has a preset width with parameter that describes the weight and its uncertainty as shown in Figure 2.1. Each parameter has a nominal value of one (1) and an increase of 10% (1.1) indicates the corresponding bin increases by 10% also. There are 50 ND and 50 SK parameters with a flux covariance matrix is shown in Figure 2.2 .

Cross Section: There are a number of cross section models and weight functions implemented in BANFF. A technical description of the models and weight functions is given in

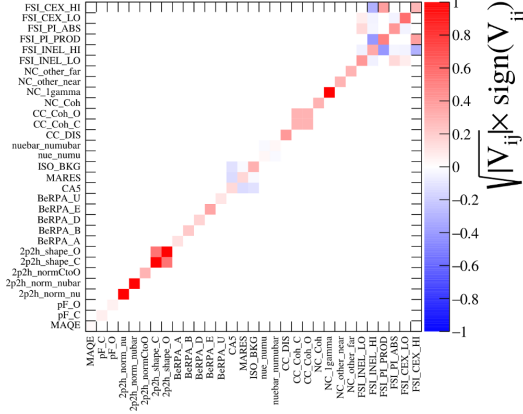


Figure 2.3: Cross section parameters pre-fit correlation matrix from the 2017 BANFF analysis.

T2K-TN-315[2]. In general, there are model parameters that describe CC- 0π , CC- 1π , FSI (FSI: final state interactions, and smaller T2K effects. There are 25 cross section parameters as shown in Figure 2.3 [1]. While most parameters are set to a nominal value of one (1), some are different like the 2p2h (MEC) parameters. Also other parameters are unconstrained like MAQE due to limitations of the dipole form factor model.

Detector Systematics: Detector systematics are implemented as normalization changes to event kinematics as well as sample migration. Variations are stored in the event-by-event response vector \vec{r} . In order to understand how the detector systematics correlate for a set of samples with varying kinematic bins, BANFF employs what are called observable normalization (obsnorm) parameters. Since the event can change from sample-to-sample and in kinematic normalization, obsnorms correlations are understood by examining how kinematics vary over many fake experiments, also called toy experiments or just toys. Therefore the nominal value for each obsnorm parameter is not one (1). The number of obsnorm parameters are determined by the analyzer by defining a set of bins that can encapsulate how events migrate across bins. A detector covariance matrix is constructed using all toy experiments. The drawback to this method is that not all detector systematics have Gaussian responses to the observables, and so the correlations are not fully accurate.

2.2 Usage of ND280 Psyche Software

Psyche is a general framework for data handling, event selections, and systematic evaluations with toy experiments. Psyche is a “lean” package from the perspective of analyzing MC events since that functionality is built heavily into Highland2. The analysis performed in this technical note required making additions to psyche in order replicate features available in Highland2. It would be wise for future analyses to build a selection in Highland2 and migrate that psyche once mature.

BANFF uses a psyche package called psycheSteering that interfaces with all the psyche tools to manage the migration of samples into its analysis code. New PØD selections were added to the psycheSelections package and validated using the psycheSteering AnalysisManager class. The AnalysisManager provides the functionality to get the true and reconstructed detector observables from each reconstructed event along with the flux tuning and detector systematic weights.

Flux tuning is the process of applying an event weight based on the true neutrino energy, flavor, and run period. Since the ND280 MC uses a series of models to describe the expected neutrino flux, it cannot perfectly model the true flux nor know the beam conditions at run time. The beam group is responsible for releasing the expected and measured neutrino flux in order to account for these differences. To flux tune an event, the relevant neutrino flavor flux histogram must be referenced. The weight is extracted by taking the ratio of the tuned flux to the nominal flux in the MC for a given neutrino energy. As an example Figure 2.4 shows the flux tuning weights for true ν_μ FHC events.

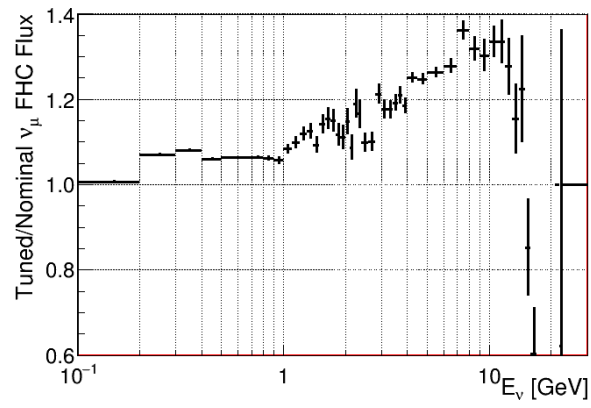


Figure 2.4: Fluxing tuning histogram for ν_μ FHC events taken from the 13av3 flux release.

3 PØD Selections and Data Samples

This section describes the development of ν_μ and $\bar{\nu}_\mu$ CC-Inclusive selections in both FHC and RHC beam configuration for PØD-based analyses. These selections are the continuation of previous works that developed ν_μ CC-Inclusive selections between the PØD and TPC1. The first such analyses were T2K-TN-80 and T2K-TN-100 which described the ν_μ CC-Inclusive event selection and, later, cross-section analysis using ND280 Production 5 software, respectively[4, 5]. These analyzes relied on each sub-detector’s reconstruction software and developed a track matching algorithm since the ND280 “Global” reconstruction matching was problematic in Production 5. As the inter-detector matching reconstruction improved in “Global”, two CC- 0π cross section analyzes, T2K-TN-258 and T2K-TN-328, were developed that also used the CC-Inclusive selection as pre-selection cuts[10, 3]. The selections described in this technical note also employ the same pre-selection cuts. What follows from here in this section is a layout of the following topic discussions.

The first topic discussed in this section is a description of the π^0 Detector (PØD). The next topic is the event reconstruction using the “Global” reconstruction software. Following that is the pre-selection cut flow. With the pre-selection cuts established, each of the three CC-Inclusive selection’s cut flow is described. Concluding this section is a discussion of the three samples in the following order: ν_μ in FHC mode, $\bar{\nu}_\mu$ in RHC, and ν_μ in RHC.

3.1 Global Reconstruction

The task of the Global reconstruction is to combine ND280 sub-detector reconstruction into an single reconstructed object. It was originally designed to analyze “CCQE-like” events in the Tracker region and has been extended with all of ND280. Global attempts to match and re-fit individual sub-detector objects using a Kalman filter while correcting for energy loss and multiscattering. A vertex associated with the re-fit object is also extracted using

Run Period	Horn Current	PØD Status	Data POT ($\times 10^{20}$)	MC POT ($\times 10^{20}$)
2	+250 kA	Water	0.4339	12.03
		Air	0.3591	9.239
3b	+205 kA		0.2172	4.478
3c	+250 kA		1.364	26.32
4			1.782	34.99
		Water	1.642	34.97
5c	-250 kA		0.4346	22.77
6b		Air	1.288	14.17
6c			0.5058	5.275
6d			0.7753	6.884
6e			0.8479	8.594
7b		Water	2.436	33.70
8	+250 kA		1.580	26.46
		Air	4.148	36.06
Sand	FHC		-	11.19
Sand	RHC		-	12.92
2, 3b, 3c, 4, 8	FHC	Air	7.872	79.18
2, 4, 8		Water	3.657	73.47
6b, 6c, 6d, 6e	RHC	Air	3.417	34.92
5c, 7b		Water	2.871	56.48

Table 3.1: T2K MC and data POT divided by run periods. The bottom four rows are the aggregated periods grouped by horn current and PØD status which is how the data analysis is performed.

a different Kalman filter. A detailed description of the track matching and vertex finding algorithms for Global is described in T2K-TN-46[9].

3.2 Data Sets

The data sets used in this analysis are runs 2-8 in both PØD water-in and water-out (air) modes as shown in Table 3.1.

3.3 PØD Selection Cuts

The selection of CC-Inclusive events use a series of cuts to select the primary lepton. The pre-selection cuts (“precuts”) are applied first to extract events that start in the PØD FV. A MIP is more likely to reach TPC1 from the PØD FV since the PØD is constructed out of heavy materials especially in the CECal. So the main track each selection is designed to select a muon.

This following sections will describe the precuts common to all CC-Inclusive selections and the branching of different cuts, after the precuts, to select the main track.

3.3.1 Pre-Selection Cuts

The pre-selection (“precuts”) were initially developed to select ν_μ CC-Inclusive using the PØD and TPC sub-detector reconstruction softwares separately[4]. They were then used with the Global reconstruction software for the ν_μ CC- 0π selection in the FHC beam configuration as described in technical note T2K-TN-258[10]. The description and flow of the precuts are described here as well since there is an incomplete description of the selection precuts.

The precuts are performed on each bunch per beam spill as follows

1. The event has a “good” data quality flag.
 - An event is rejected if any sub-detector or electronics in ND280 reported as “bad” during that bunch.
2. There is at least one (1) track reconstructed in TPC1.
 - There are no restrictions on the number of tracks fully contained in the PØD or exiting into other sub-detectors.
3. The track in TPC1 must have more than 18 nodes.

- The TPC reconstruction gathers vertical and horizontal hits into clusters of hits. The charge distribution of the cluster is used to get a vertical (horizontal) position that is more accurate than the individual readout pads. A node is constructed out of each cluster with associated track state information. The set of nodes are used to fit the track helix[8].

4. The reconstructed vertex is within the PØD WT FV.

- The PØD FV is defined to include as much as the WT regions as possible. Its X and Y borders are 25 cm away from the PØDule edges while its Z borders intersect the last and first half downstream PØDule in the USECal and CECal, respectively. The enumerated volume edges are shown in table 3.2. This volume, while used for track-based analyzes in the past, was optimized for π^0 and ν_e analyzes[6].

5. All tracks that enter TPC1 pass the veto cut

- An event is rejected if any PØD track enters TPC1 from outside the “corridor” volume. This cut was designed to eliminate broken tracks between the PØD and TPC1 when the separate sub-detector reconstructions were used[4]. In practice, this cut ensures that Global tracks entering TPC1 away from its X and Y edges. The corridor definition is the same as defined in T2K-TN-208 and shown in Table 3.2.

PØD WT FV			Corridor Volume		
-836	< X <	764	-988	< X <	910
-871	< Y <	869	-1020	< Y <	1010
-2969	< Z <	1264	-3139	< Z <	-900

Table 3.2: The PØD WT FV (left) and veto corridor volume (right) in the ND280 coordinate system. The corridor spans from the 5th (8th) to 40th (80th) PØDule (scintillator layer). All the units are given in millimeters.

After passing all the precuts, a single, global track, which is observed in TPC1, is assigned as the “main track” of a selection. The main track for ν_μ selections is the highest momentum, negatively-charged track (HMNT). Similarly the highest momentum, positively-charged track (HMPT) is assigned the main track for $\bar{\nu}_\mu$ selections.

This concludes the application of precuts to all the CC-Inclusive selections. The following subsections describe the CC-Inclusive selection cuts, first in FHC mode and then RHC mode.

3.3.2 CC-Inclusive in FHC

As discussed in Section section 3.3.1 on page 18, this selection is the basis for the ν_μ CC-0 π PØD+TPC1 analysis. This is FHC mode selection and so the lack of a negatively charged track is the final cut for the CC-Inclusive selection.

3.3.3 CC-Inclusive in RHC

3.4 PØD Water-Out Samples

This section shows the kinematic distributions for the PØD water-out samples. First an examination of the CC-Inclusive samples and the effects of the systematic weights will be explored. The samples are then examined as CC 1-track and CC N-tracks.

3.4.1 CC-Inclusive

The CC-Inclusive sample cuts are discussed 3.3.1. Since both flux and systematic weights are applied to all MC events in BANFF, it is important to validate the event weights. Using neither set of weights is referred to as the nominal MC.

ν_μ **FHC**: Shown in Figures 3.1 to 3.7 are the momentum and $\cos \theta$ distributions for ν_μ CC-Inclusive events in FHC mode. There are three pairs of P, θ figures with the same truth information break down accompanied by one of neutrino energy. The truth information categories are lepton candidate particle, NEUT reaction, and topology. Each figure consists of a set of four sub-figures which illustrate the application of flux and detector systematic weights.

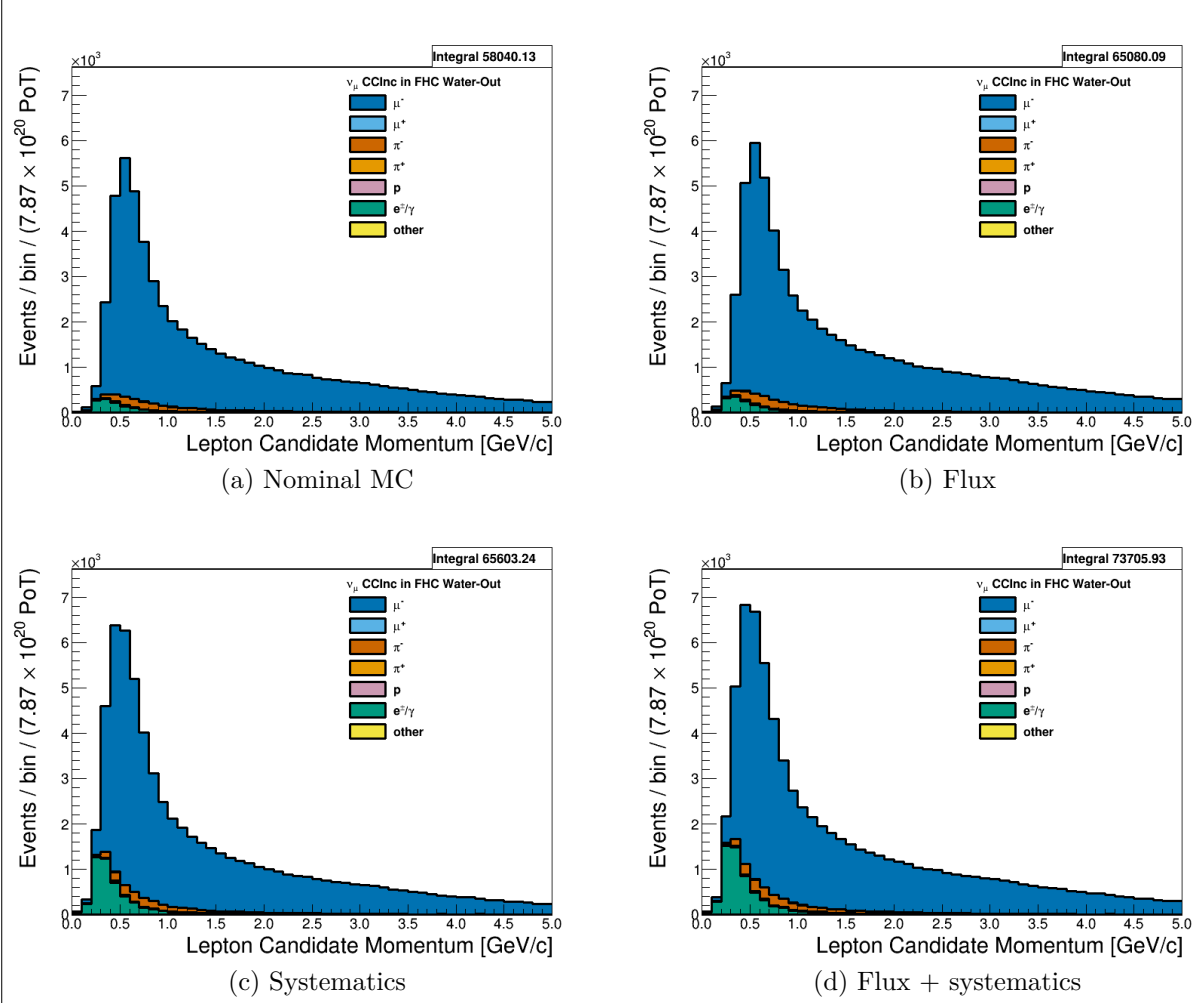


Figure 3.1: Reconstructed lepton candidate momentum separated by true particle species for FHC ν_μ CC-Inc. events occurring in the PØD in water-out mode. (a) The nominal MC prediction without any weights applied. (b) The flux tuning is applied. (c) The systematic weighting is applied. (d) Both flux and systematic weighting is applied.

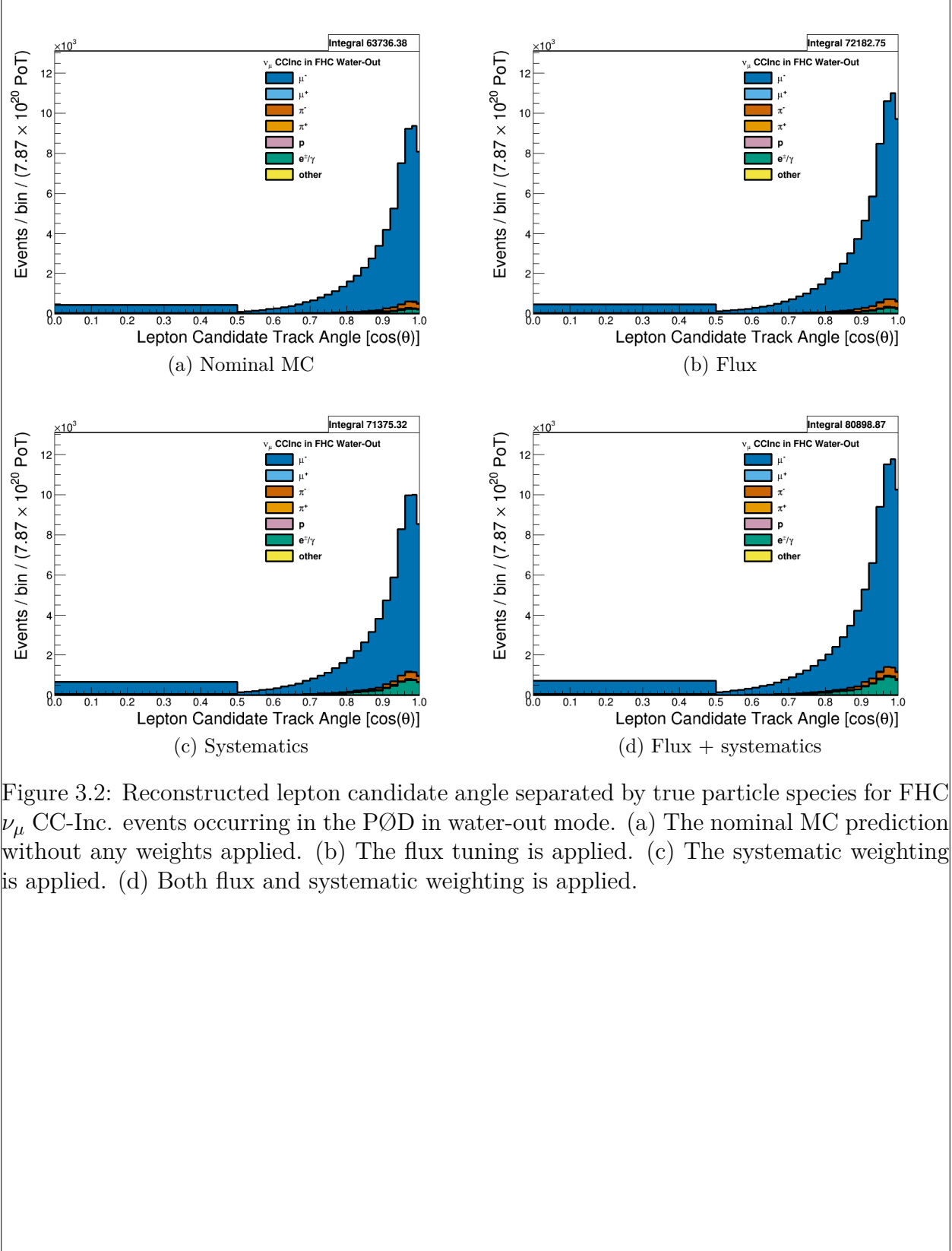


Figure 3.2: Reconstructed lepton candidate angle separated by true particle species for FHC ν_μ CC-Inc. events occurring in the PØD in water-out mode. (a) The nominal MC prediction without any weights applied. (b) The flux tuning is applied. (c) The systematic weighting is applied. (d) Both flux and systematic weighting is applied.

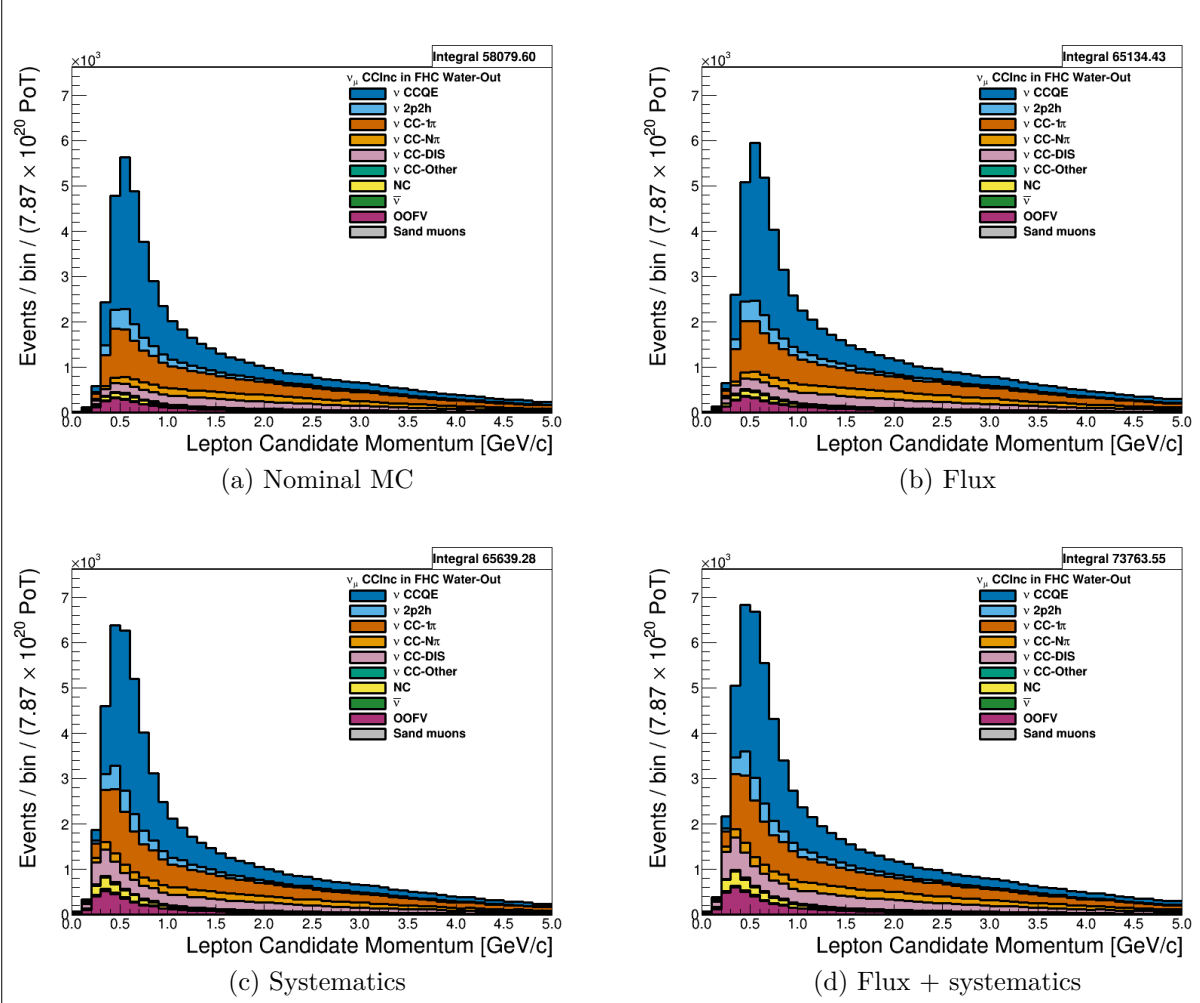


Figure 3.3: Reconstructed lepton candidate momentum separated by NEUT model interaction mode for FHC ν_μ CC-Inc. events occurring in the PØD in water-out mode. (a) The nominal MC prediction without any weights applied. (b) The flux tuning is applied. (c) The systematic weighting is applied. (d) Both flux and systematic weighting is applied.

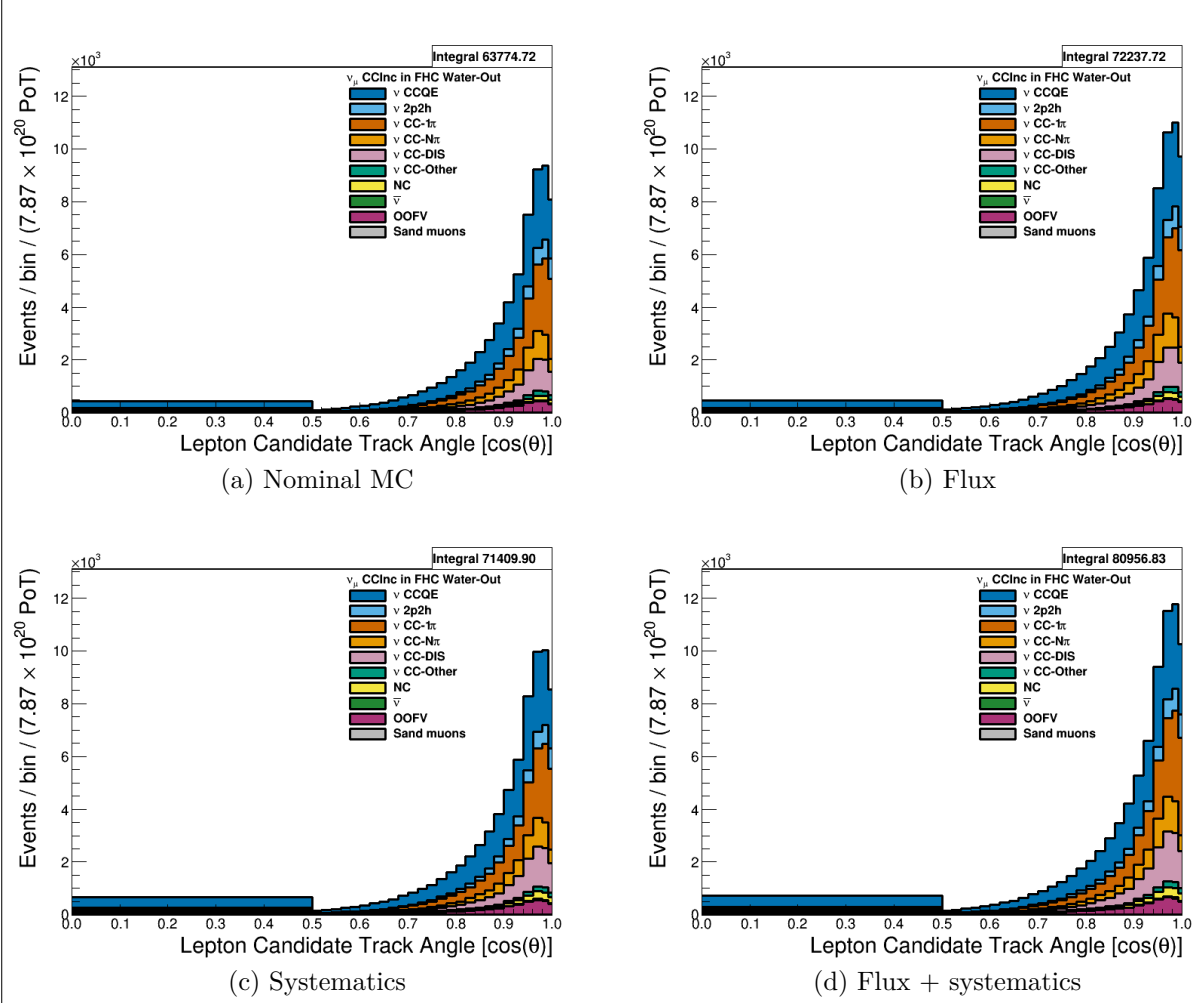


Figure 3.4: Reconstructed lepton candidate $\cos\theta$ separated by NEUT model interaction mode for FHC ν_μ CC-Inc. events occurring in the PØD in water-out mode. (a) The nominal MC prediction without any weights applied. (b) The flux tuning is applied. (c) The systematic weighting is applied. (d) Both flux and systematic weighting is applied.

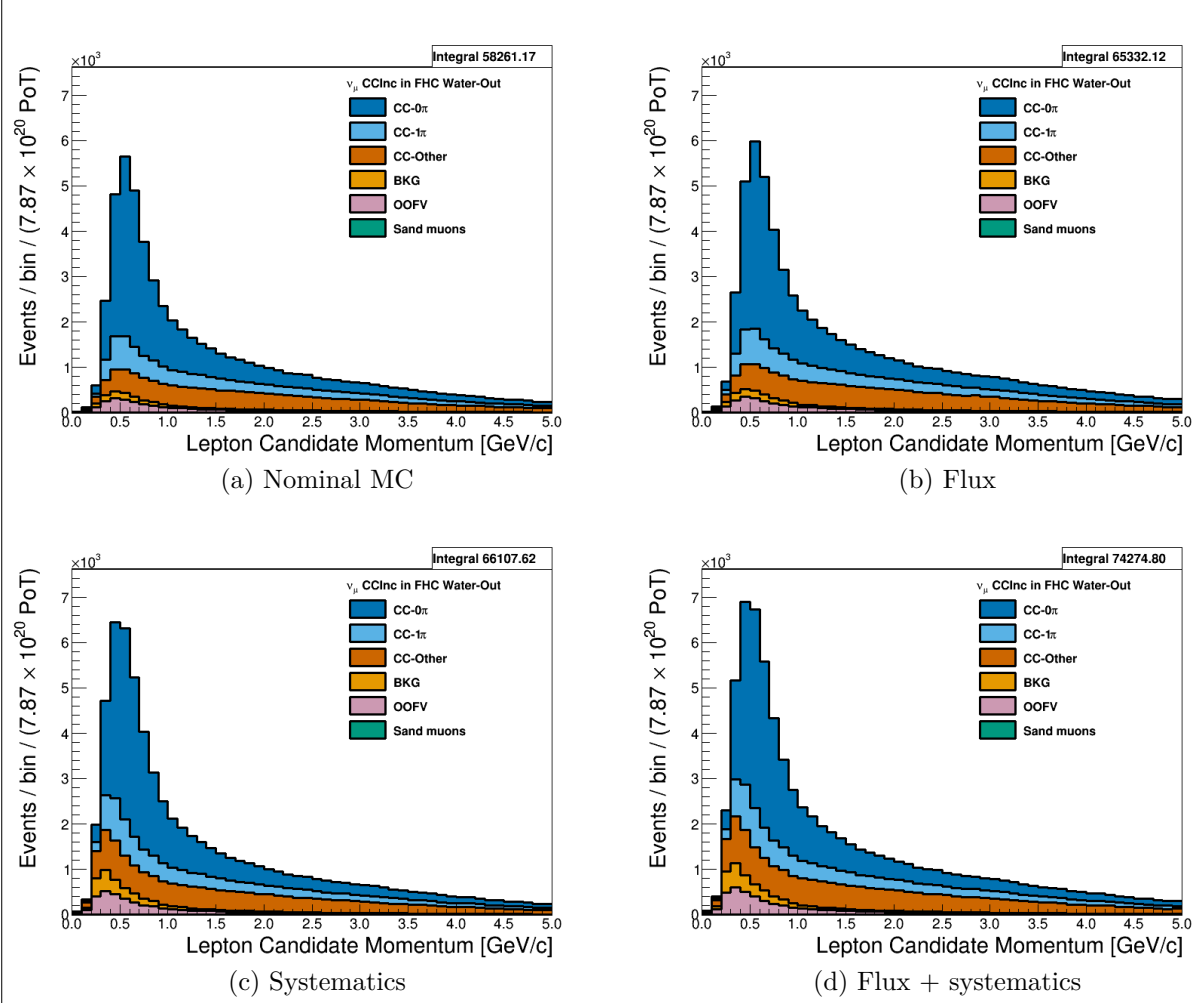


Figure 3.5: Reconstructed lepton candidate momentum separated by topology for FHC ν_μ CC-Inc. events occurring in the PØD in water-out mode. (a) The nominal MC prediction without any weights applied. (b) The flux tuning is applied. (c) The systematic weighting is applied. (d) Both flux and systematic weighting is applied.

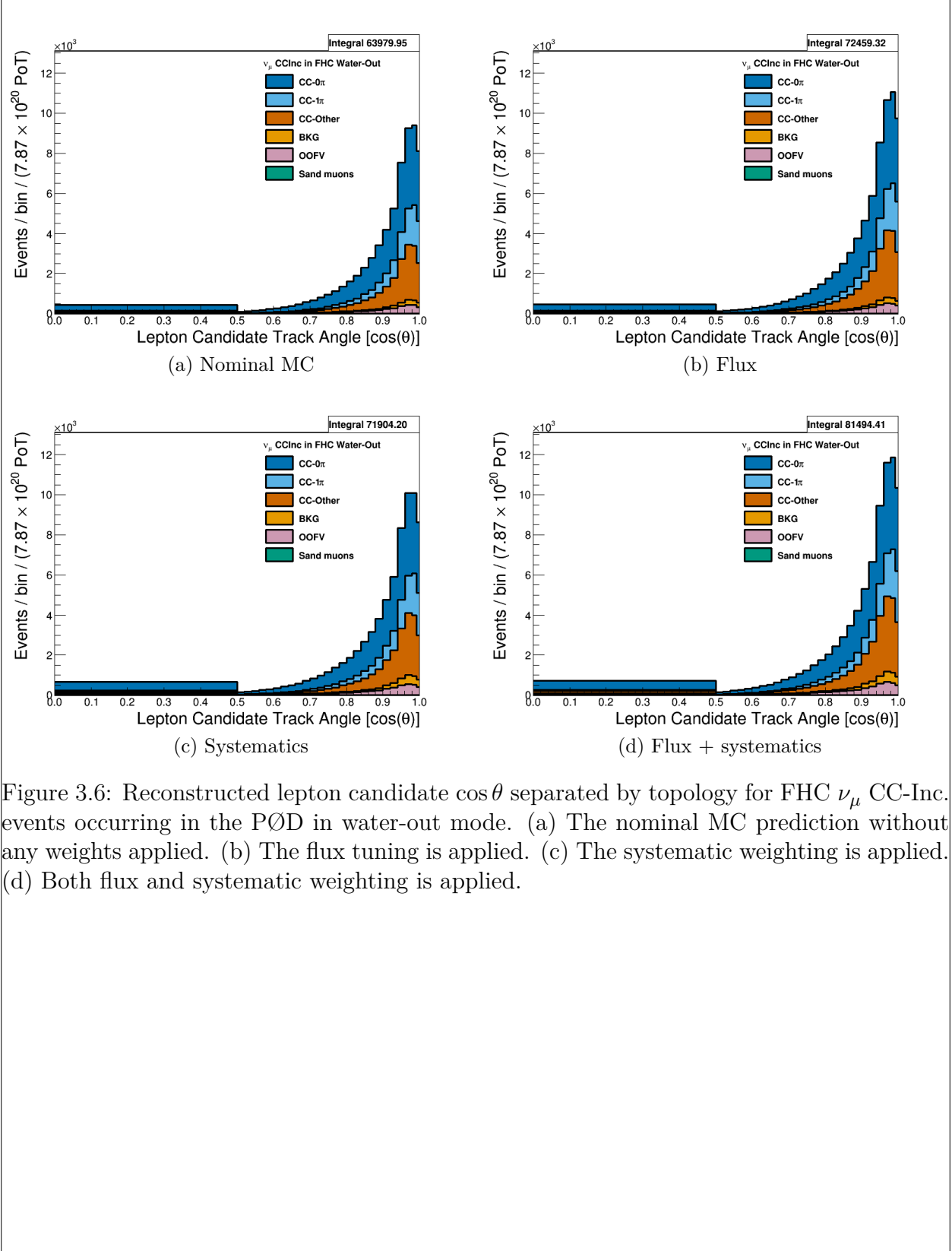


Figure 3.6: Reconstructed lepton candidate $\cos\theta$ separated by topology for FHC ν_μ CC-Inc. events occurring in the PØD in water-out mode. (a) The nominal MC prediction without any weights applied. (b) The flux tuning is applied. (c) The systematic weighting is applied. (d) Both flux and systematic weighting is applied.

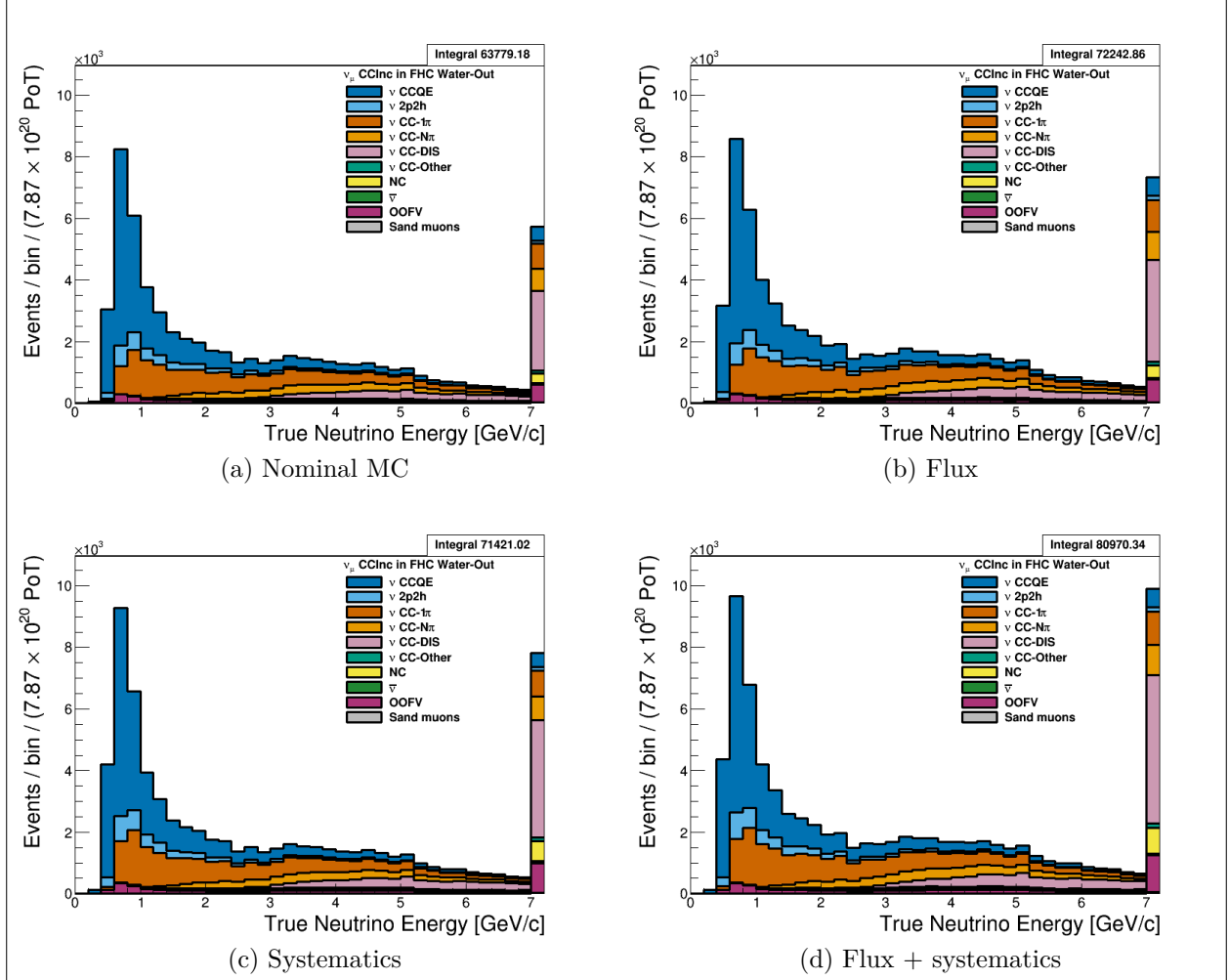


Figure 3.7: True neutrino energy associated with the lepton candidate separated by NEUT model interaction mode for FHC ν_μ CC-Inc. events occurring in the PØD in water-out mode. (a) The nominal MC prediction without any weights applied. (b) The flux tuning is applied. (c) The systematic weighting is applied. (d) Both flux and systematic weighting is applied.

$\bar{\nu}_\mu$ **RHC**: Shown in Figures 3.8 to 3.14 for $\bar{\nu}_\mu$ CC-Inclusive events in RHC mode. There are three pairs of P, θ figures with the same truth information break down accompanied by one of neutrino energy. The truth information categories are lepton candidate particle, NEUT reaction, and topology. Each figure consists of a set of four sub-figures which illustrate the application of flux and detector systematic weights.

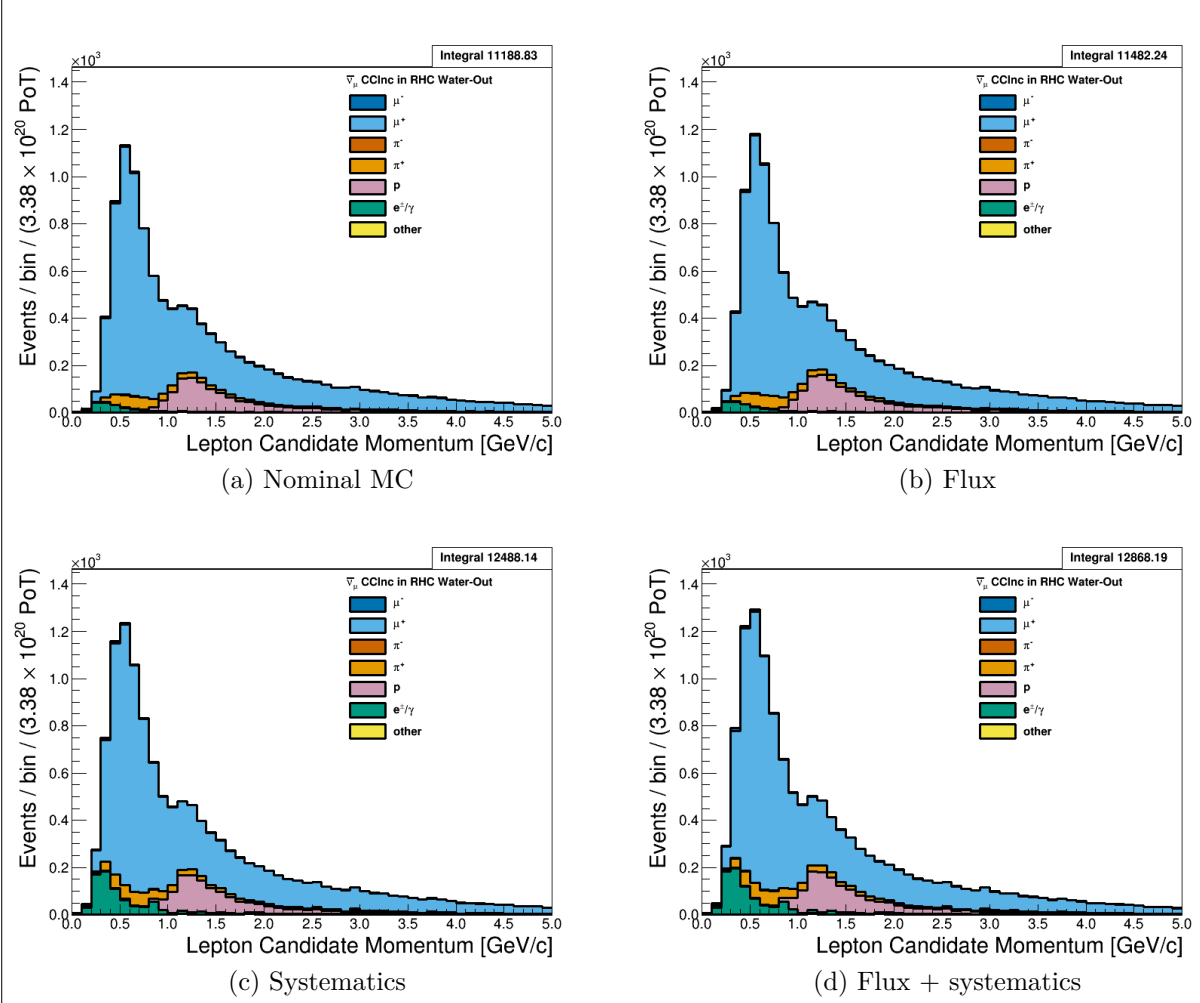


Figure 3.8: Reconstructed lepton candidate momentum separated by true particle species for RHC $\bar{\nu}_\mu$ CC-Inc. events occurring in the PØD in water-out mode. (a) The nominal MC prediction without any weights applied. (b) The flux tuning is applied. (c) The systematic weighting is applied. (d) Both flux and systematic weighting is applied.

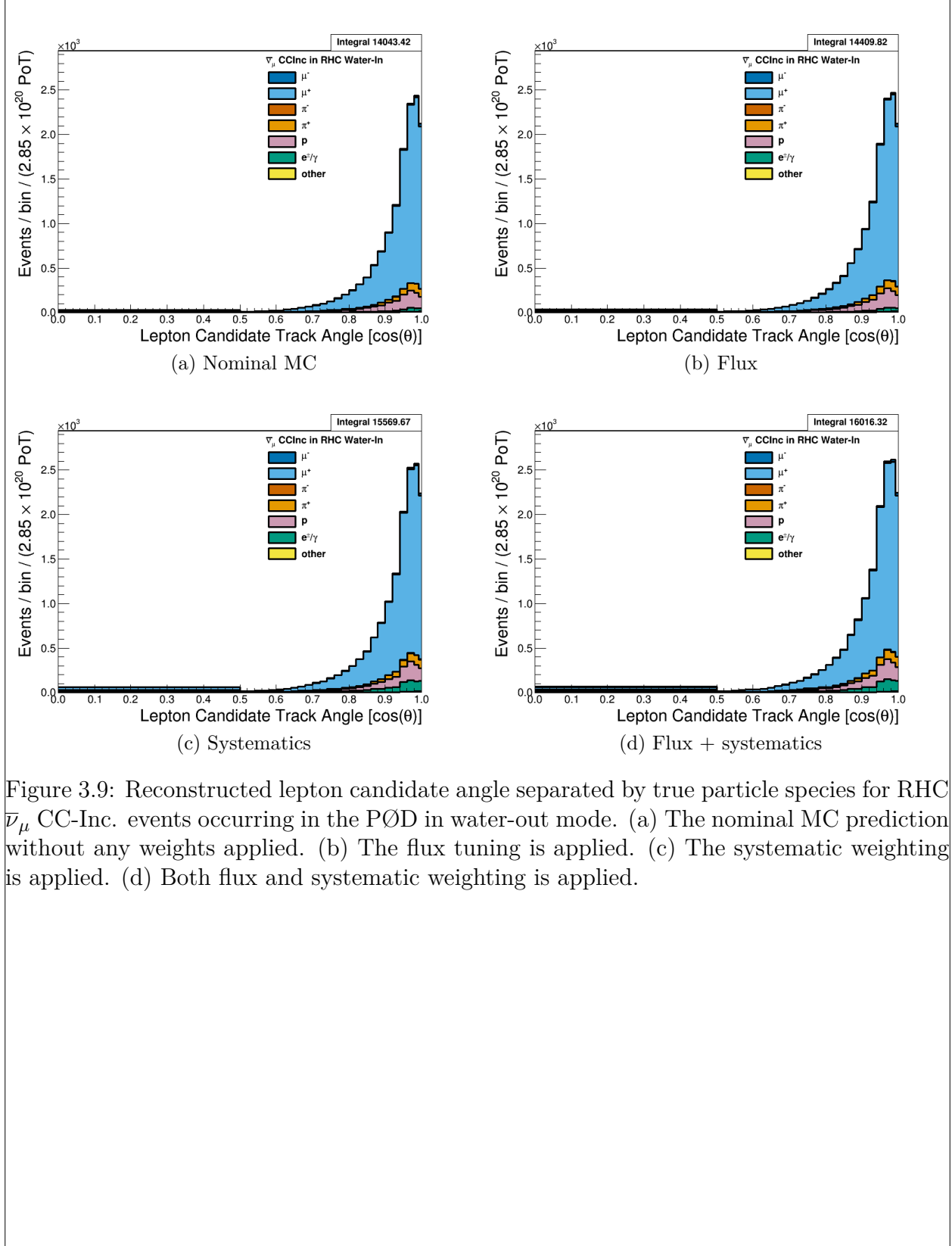


Figure 3.9: Reconstructed lepton candidate angle separated by true particle species for RHC $\bar{\nu}_\mu$ CC-Inc. events occurring in the PØD in water-out mode. (a) The nominal MC prediction without any weights applied. (b) The flux tuning is applied. (c) The systematic weighting is applied. (d) Both flux and systematic weighting is applied.

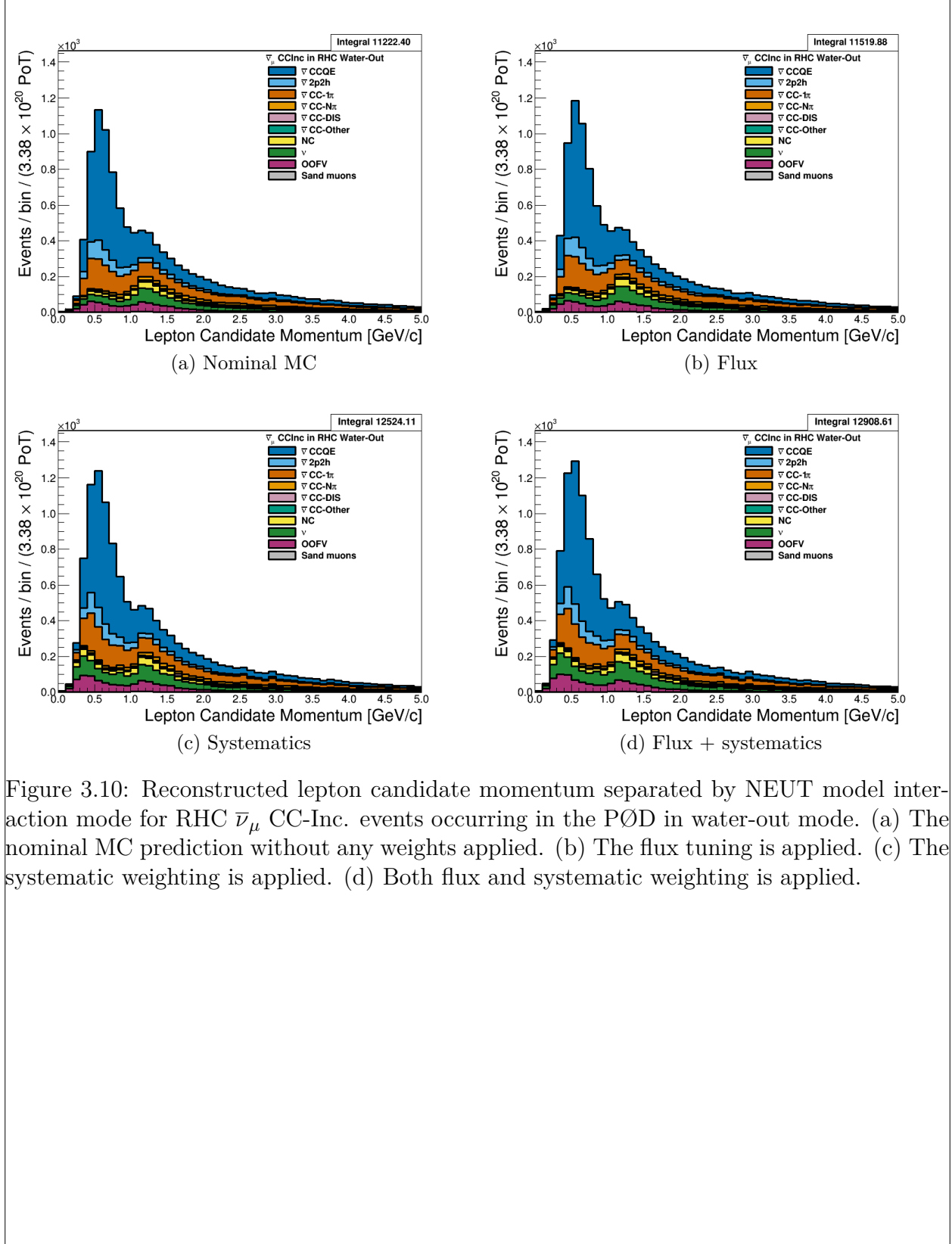


Figure 3.10: Reconstructed lepton candidate momentum separated by NEUT model interaction mode for RHC $\bar{\nu}_\mu$ CC-Inc. events occurring in the PØD in water-out mode. (a) The nominal MC prediction without any weights applied. (b) The flux tuning is applied. (c) The systematic weighting is applied. (d) Both flux and systematic weighting is applied.

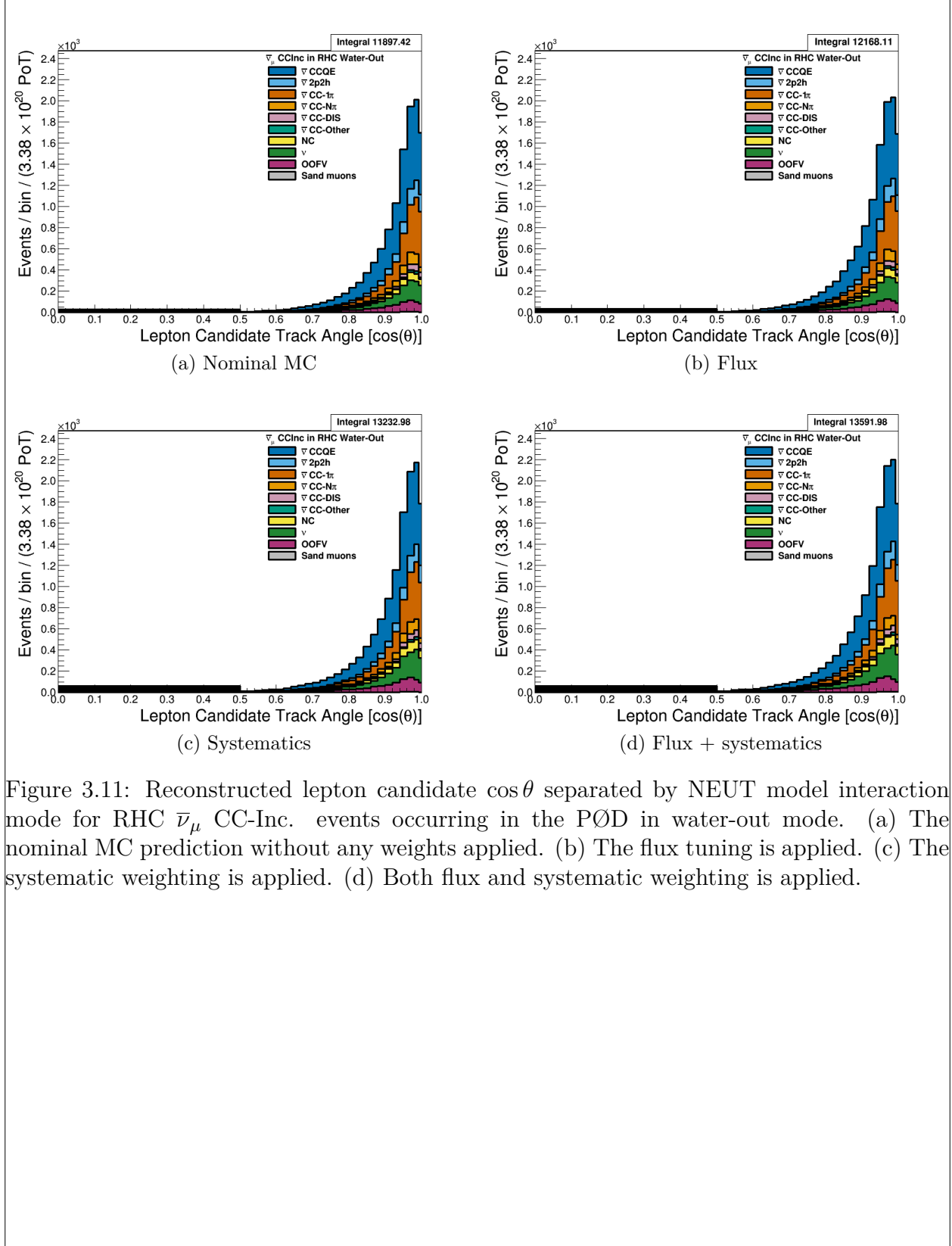


Figure 3.11: Reconstructed lepton candidate $\cos\theta$ separated by NEUT model interaction mode for RHC $\bar{\nu}_\mu$ CC-Inc. events occurring in the PØD in water-out mode. (a) The nominal MC prediction without any weights applied. (b) The flux tuning is applied. (c) The systematic weighting is applied. (d) Both flux and systematic weighting is applied.

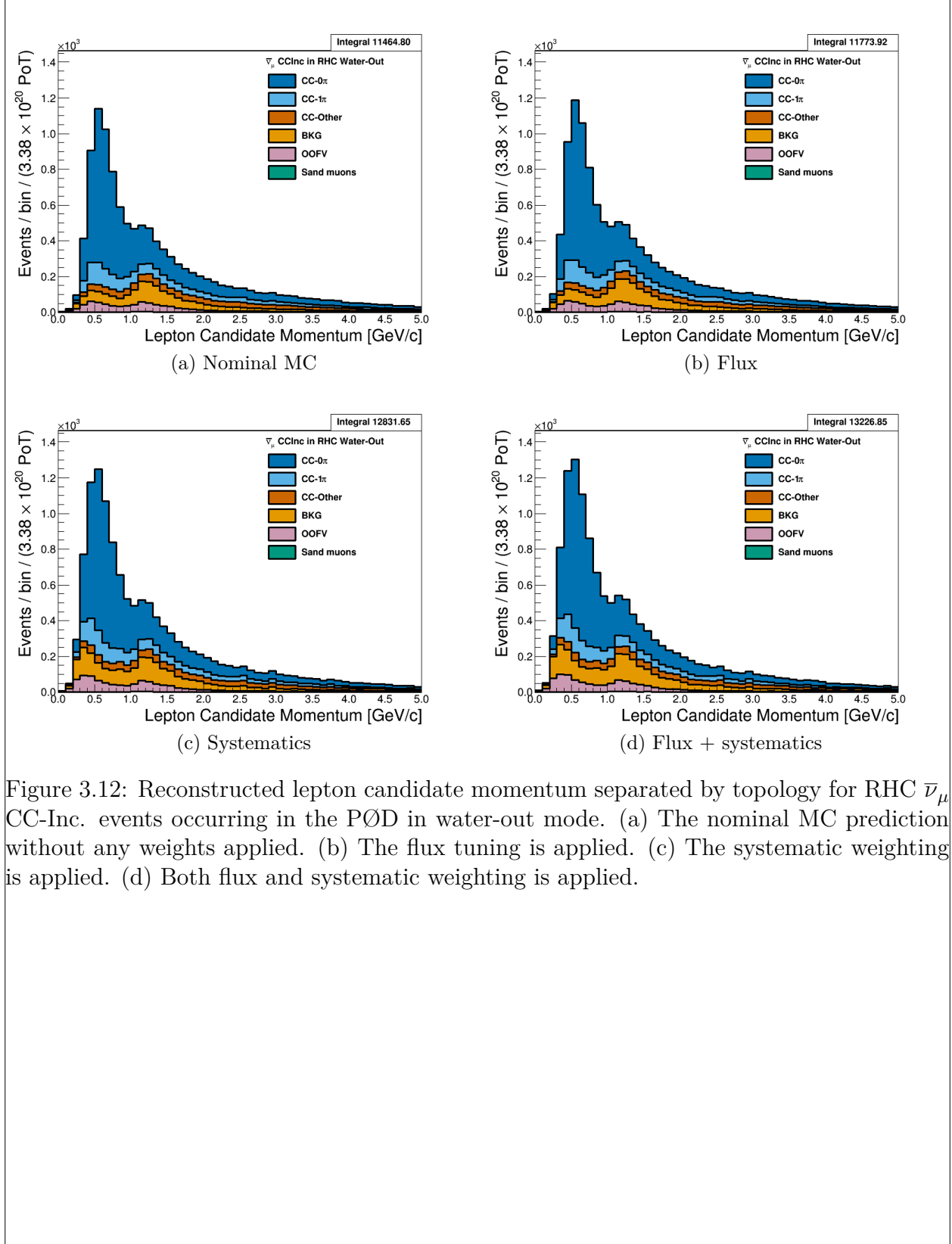


Figure 3.12: Reconstructed lepton candidate momentum separated by topology for RHC $\bar{\nu}_\mu$ CC-Inc. events occurring in the PØD in water-out mode. (a) The nominal MC prediction without any weights applied. (b) The flux tuning is applied. (c) The systematic weighting is applied. (d) Both flux and systematic weighting is applied.

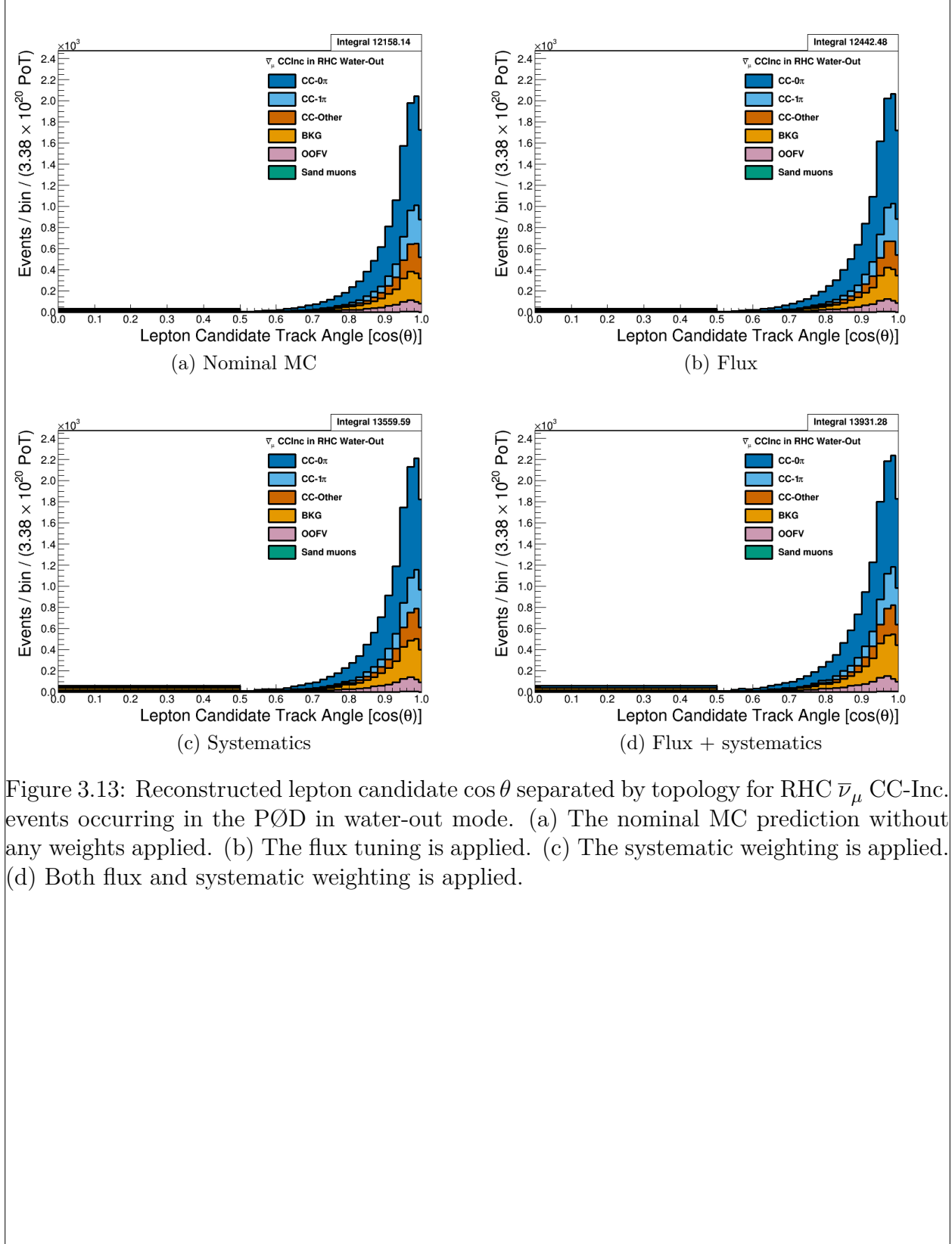


Figure 3.13: Reconstructed lepton candidate $\cos\theta$ separated by topology for RHC $\bar{\nu}_\mu$ CC-Inc. events occurring in the PØD in water-out mode. (a) The nominal MC prediction without any weights applied. (b) The flux tuning is applied. (c) The systematic weighting is applied. (d) Both flux and systematic weighting is applied.

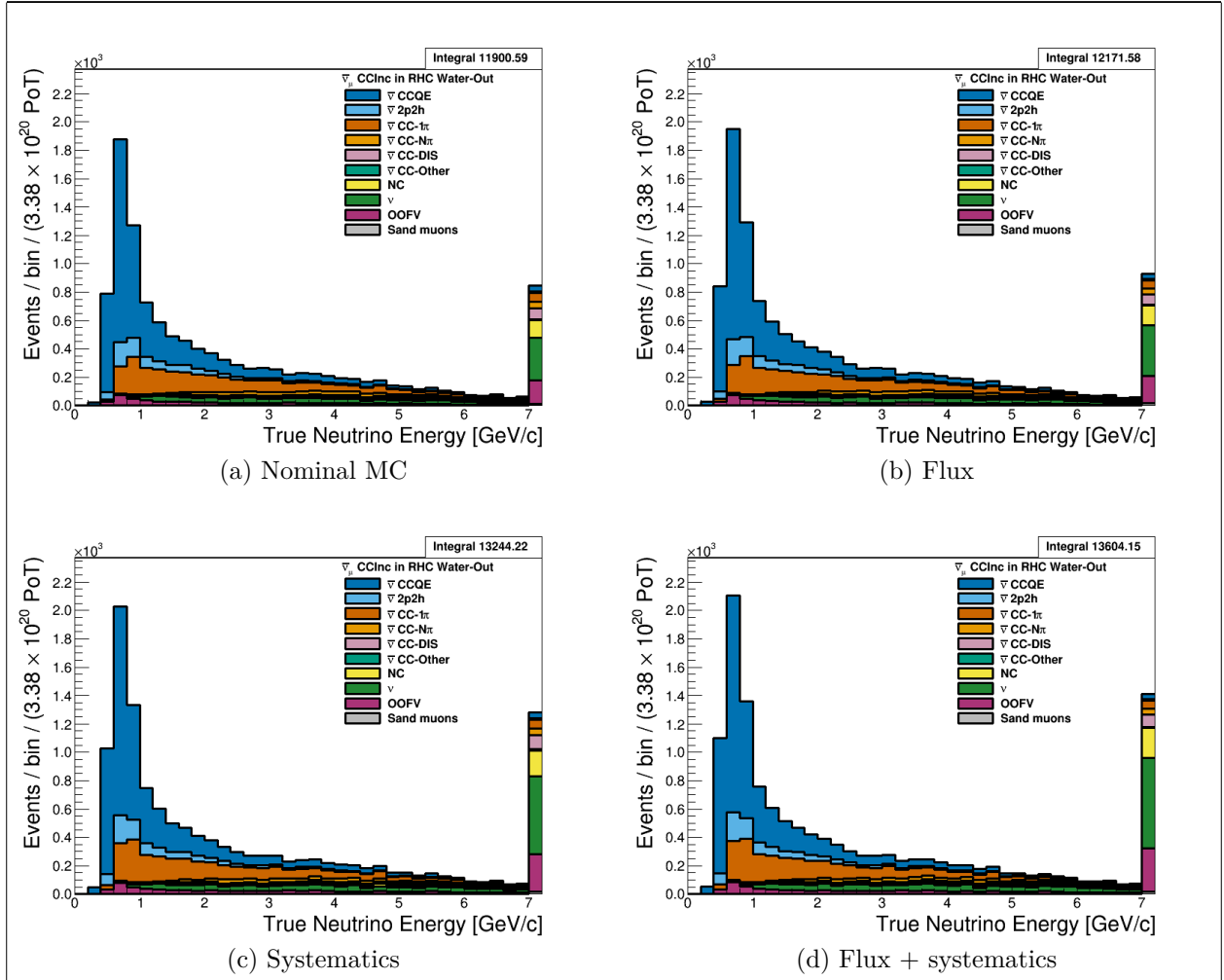


Figure 3.14: True neutrino energy associated with the lepton candidate separated by NEUT model interaction mode for RHC $\bar{\nu}_\mu$ CC-Inc. events occurring in the PØD in water-out mode. (a) The nominal MC prediction without any weights applied. (b) The flux tuning is applied. (c) The systematic weighting is applied. (d) Both flux and systematic weighting is applied.

ν_μ RHC: Add figures here

3.4.2 CC-1 Track (CCQE Enhanced)

Add figures here

3.4.3 CC-N Tracks (CCnQE Enhanced)

Add figures here

3.5 PØD Water-In Samples

This section shows the kinematic distributions for the PØD water-in samples. These samples will demonstrate the similarities between it and water-out modes. First an examination of the CC-Inclusive samples and the effects of the systematic weights will be explored. The samples are then examined as CC 1-track and CC N-tracks.

3.5.1 CC-Inclusive

The CC-Inclusive sample cuts are discussed 3.3.1. Since both flux and detector systematic weights are applied to all MC events in BANFF, it is important to validate the event weights. Using neither set of weights is referred to as the nominal MC.

ν_μ **FHC**: Shown in Figures 3.15 to 3.21 are the momentum and $\cos\theta$ distributions for ν_μ CC-Inclusive events in FHC mode. There are three pairs of P, θ figures with the same truth information break down accompanied by one of neutrino energy. The truth information categories are lepton candidate particle, NEUT reaction, and topology. Each figure consists of a set of four sub-figures which illustrate the application of flux and detector systematic weights.

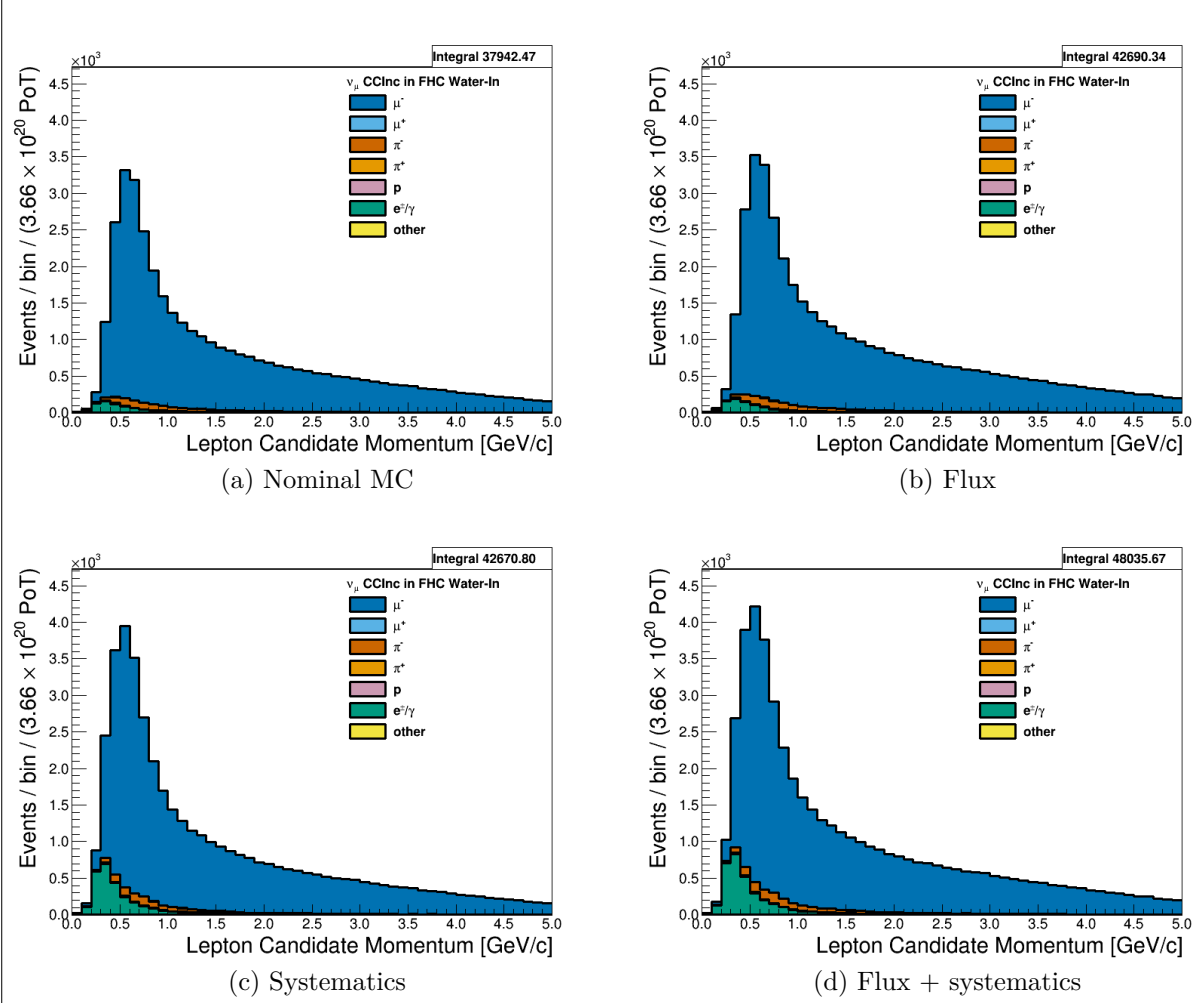


Figure 3.15: Reconstructed lepton candidate momentum separated by true particle species for FHC ν_μ CC-Inc. events occurring in the PØD in water-in mode. (a) The nominal MC prediction without any weights applied. (b) The flux tuning is applied. (c) The systematic weighting is applied. (d) Both flux and systematic weighting is applied.

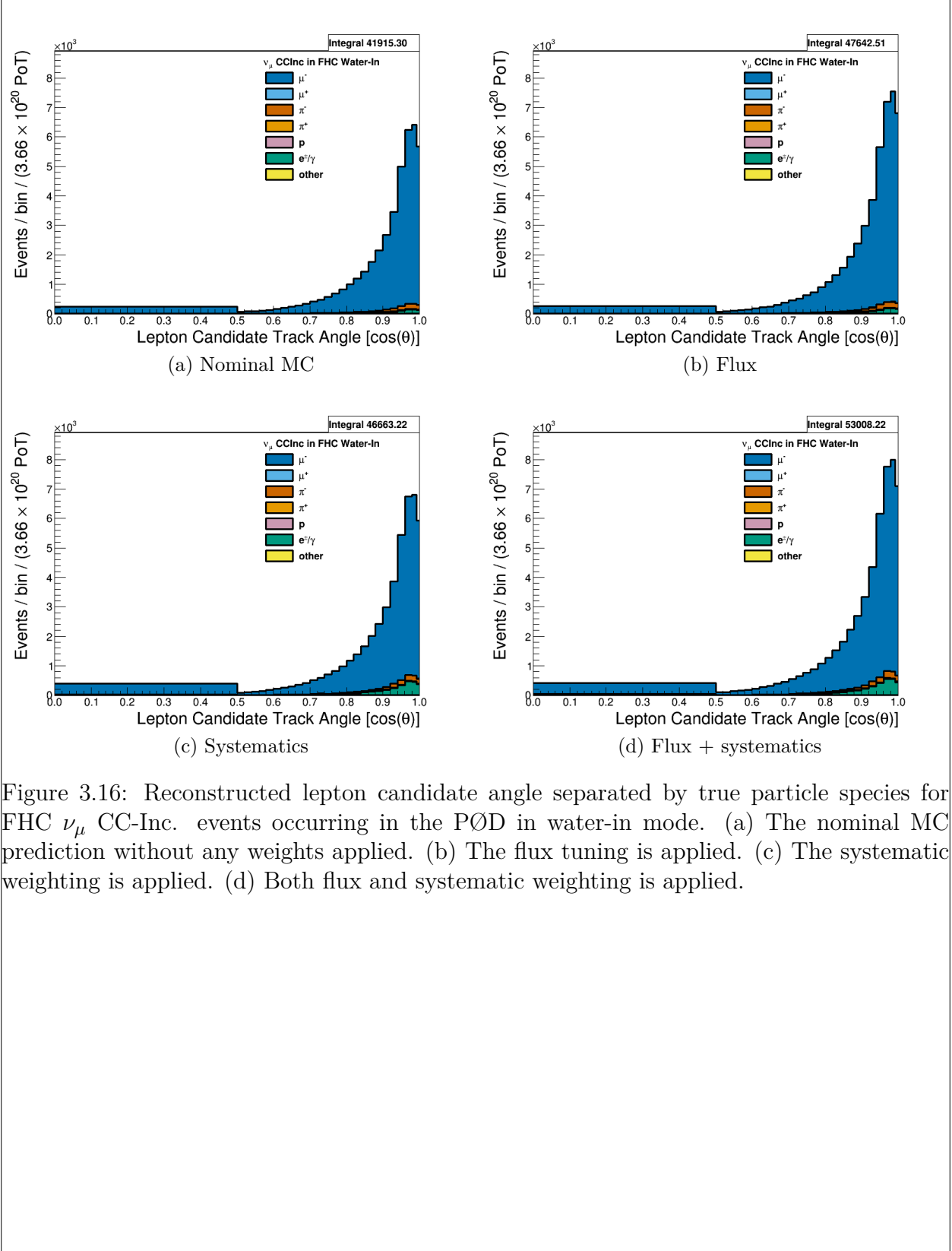


Figure 3.16: Reconstructed lepton candidate angle separated by true particle species for FHC ν_μ CC-Inc. events occurring in the PØD in water-in mode. (a) The nominal MC prediction without any weights applied. (b) The flux tuning is applied. (c) The systematic weighting is applied. (d) Both flux and systematic weighting is applied.

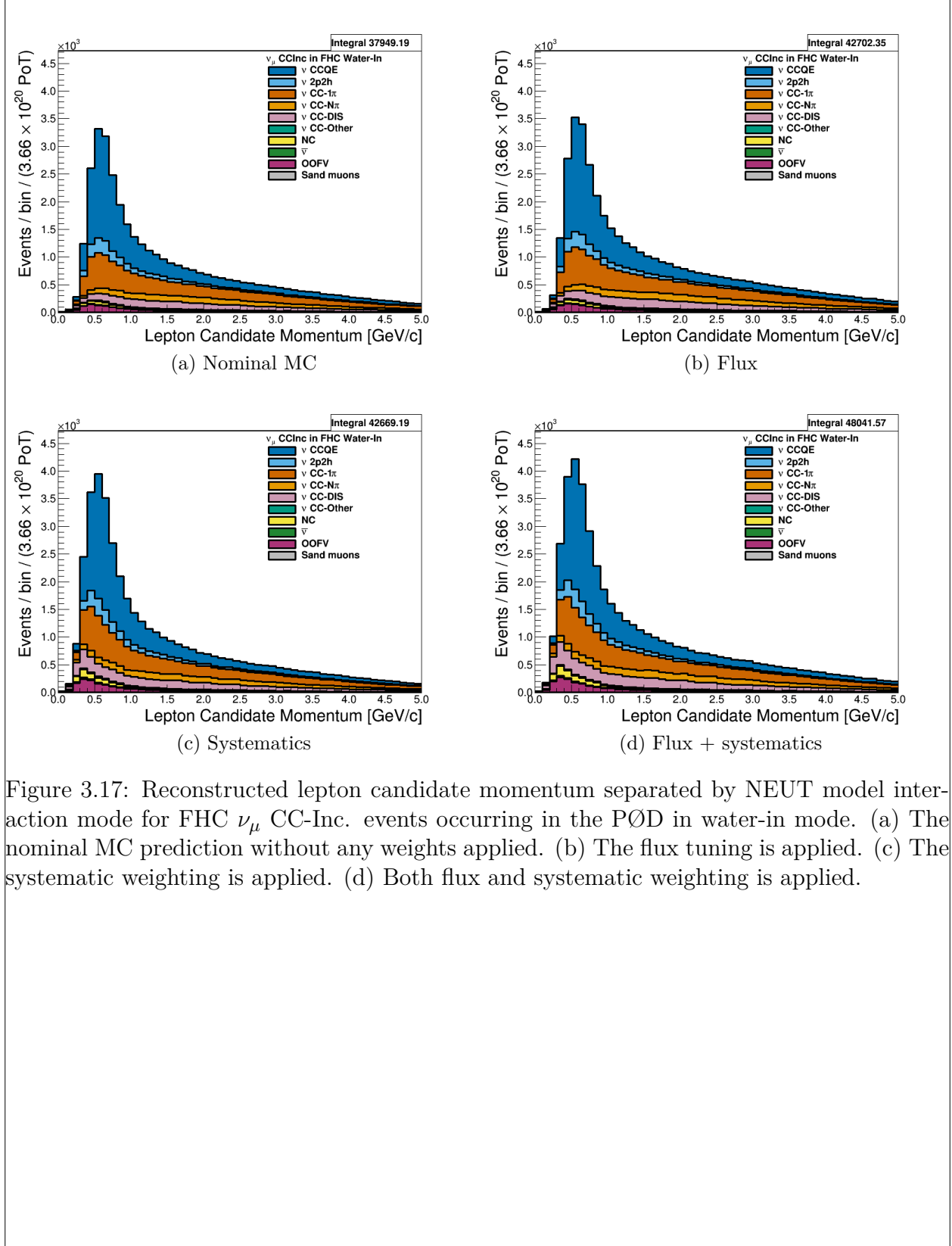


Figure 3.17: Reconstructed lepton candidate momentum separated by NEUT model interaction mode for FHC ν_μ CC-Inc. events occurring in the PØD in water-in mode. (a) The nominal MC prediction without any weights applied. (b) The flux tuning is applied. (c) The systematic weighting is applied. (d) Both flux and systematic weighting is applied.

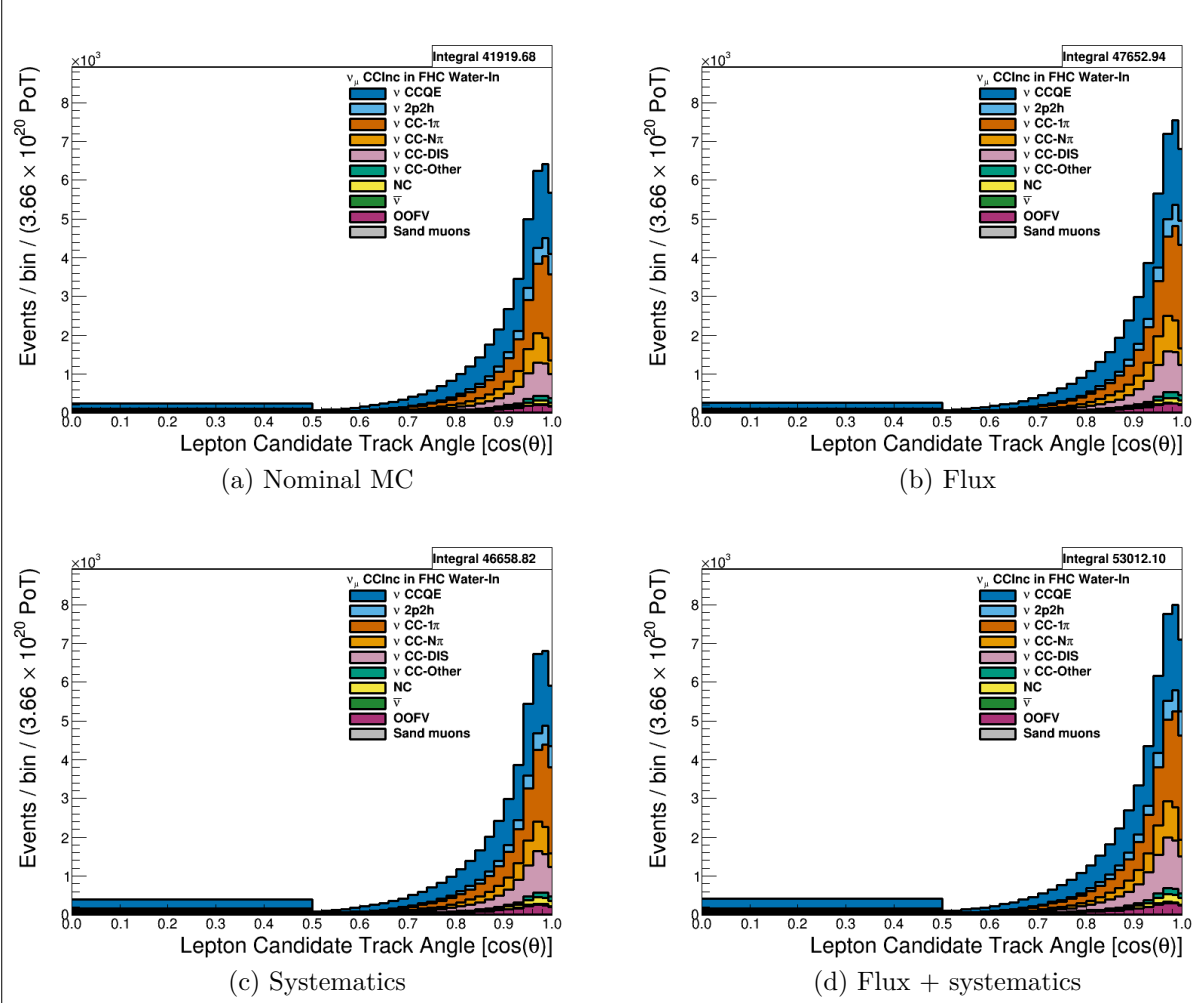


Figure 3.18: Reconstructed lepton candidate $\cos\theta$ separated by NEUT model interaction mode for FHC ν_μ CC-Inc. events occurring in the PØD in water-in mode. (a) The nominal MC prediction without any weights applied. (b) The flux tuning is applied. (c) The systematic weighting is applied. (d) Both flux and systematic weighting is applied.

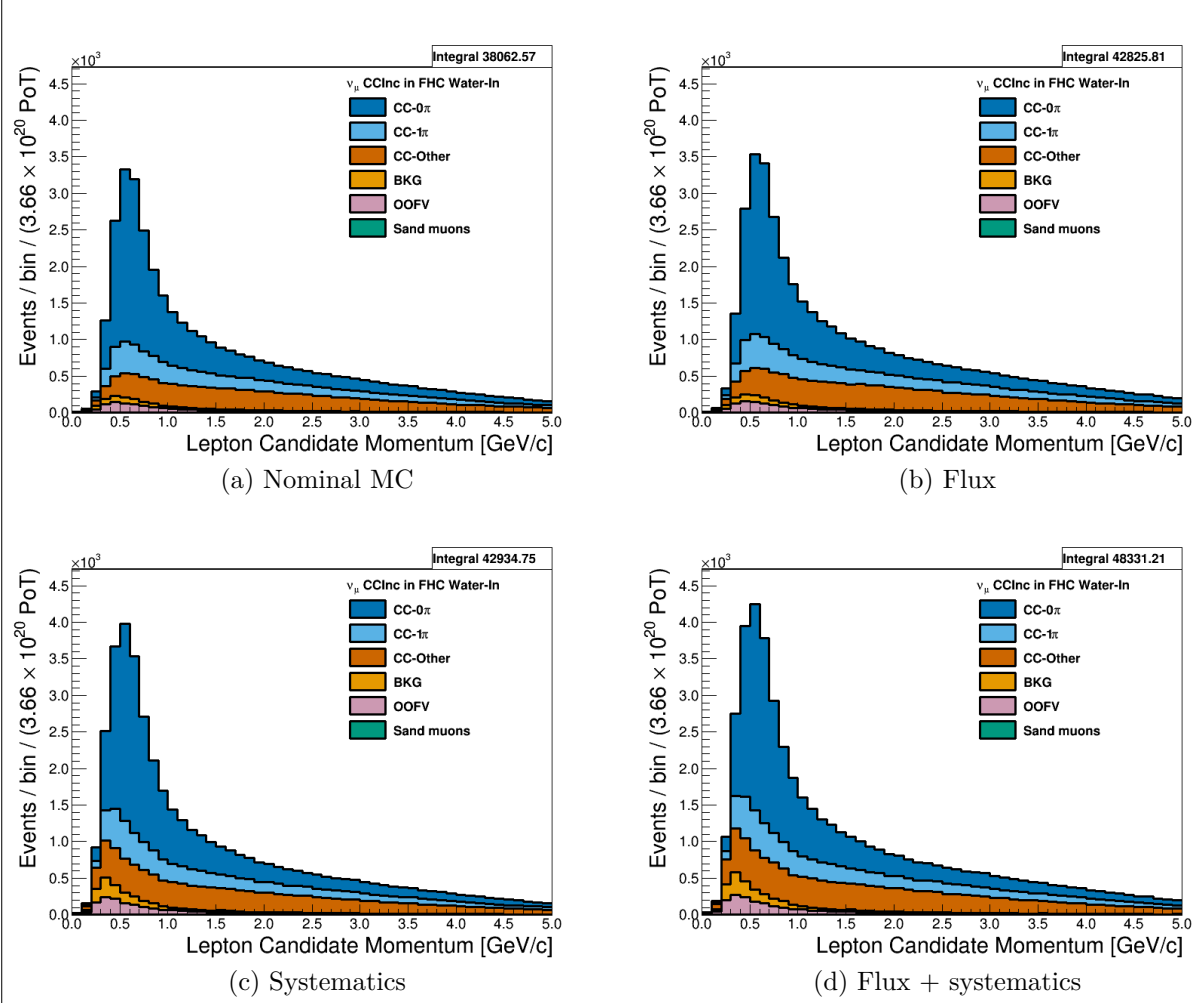


Figure 3.19: Reconstructed lepton candidate momentum separated by topology for FHC ν_μ CC-Inc. events occurring in the PØD in water-in mode. (a) The nominal MC prediction without any weights applied. (b) The flux tuning is applied. (c) The systematic weighting is applied. (d) Both flux and systematic weighting is applied.

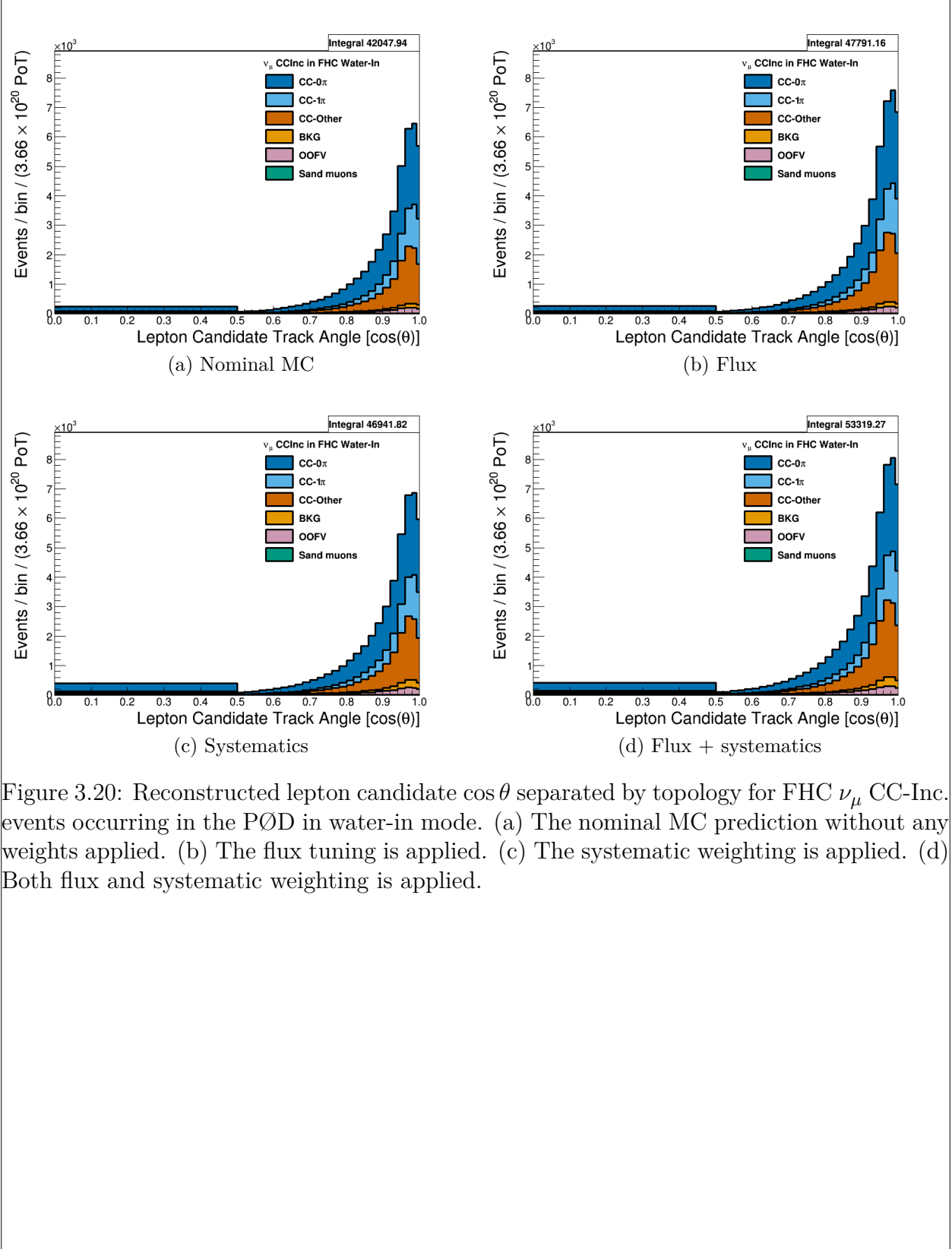


Figure 3.20: Reconstructed lepton candidate $\cos\theta$ separated by topology for FHC ν_μ CC-Inc. events occurring in the PØD in water-in mode. (a) The nominal MC prediction without any weights applied. (b) The flux tuning is applied. (c) The systematic weighting is applied. (d) Both flux and systematic weighting is applied.

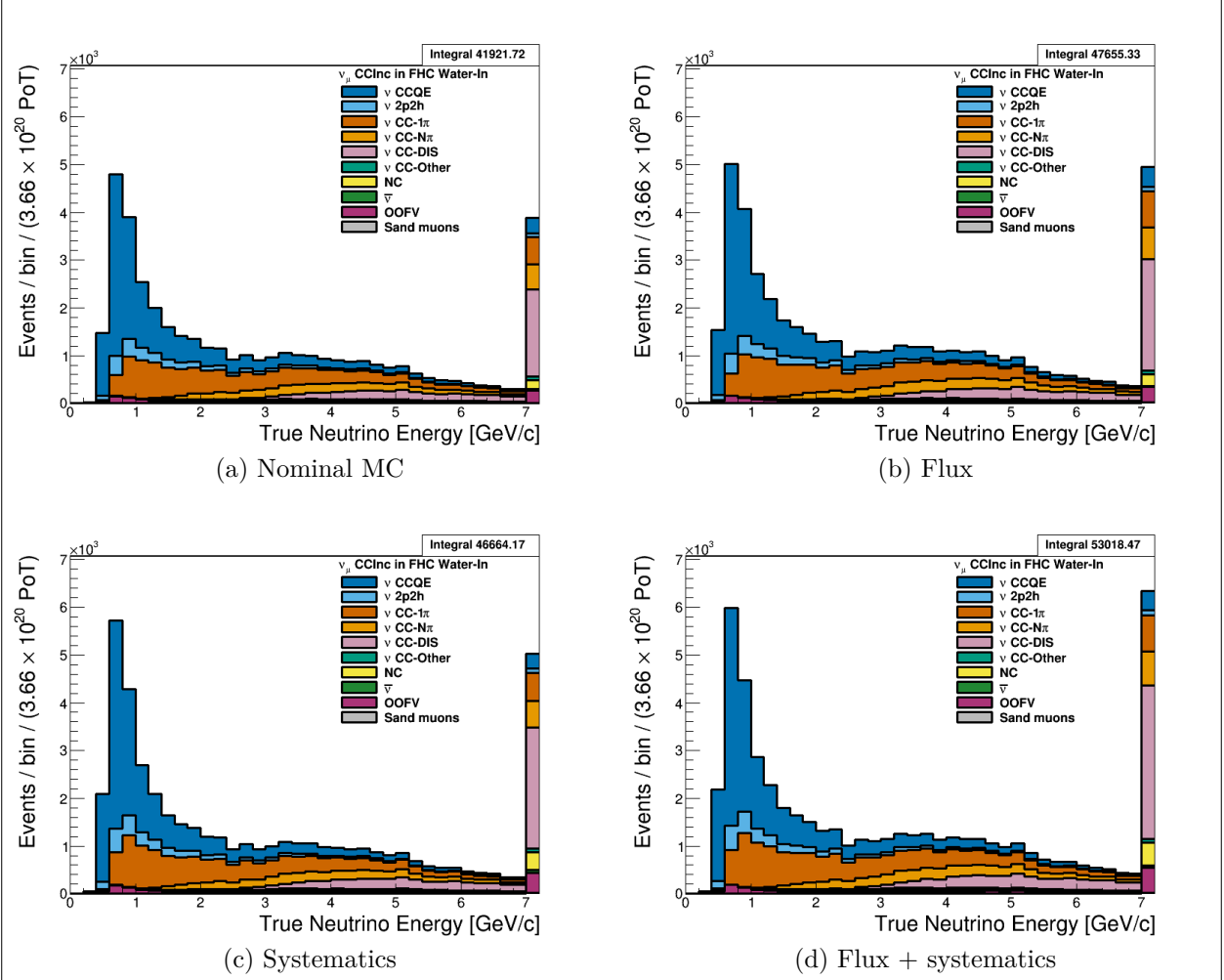


Figure 3.21: True neutrino energy associated with the lepton candidate separated by NEUT model interaction mode for FHC ν_μ CC-Inc. events occurring in the PØD in water-out mode. (a) The nominal MC prediction without any weights applied. (b) The flux tuning is applied. (c) The systematic weighting is applied. (d) Both flux and systematic weighting is applied.

$\bar{\nu}_\mu$ **RHC**: Shown in Figures 3.22 to 3.28 for $\bar{\nu}_\mu$ CC-Inclusive events in RHC mode. There are three pairs of P, θ figures with the same truth information break down accompanied by one of neutrino energy. The truth information categories are lepton candidate particle, NEUT reaction, and topology. Each figure consists of a set of four sub-figures which illustrate the application of flux and detector systematic weights.

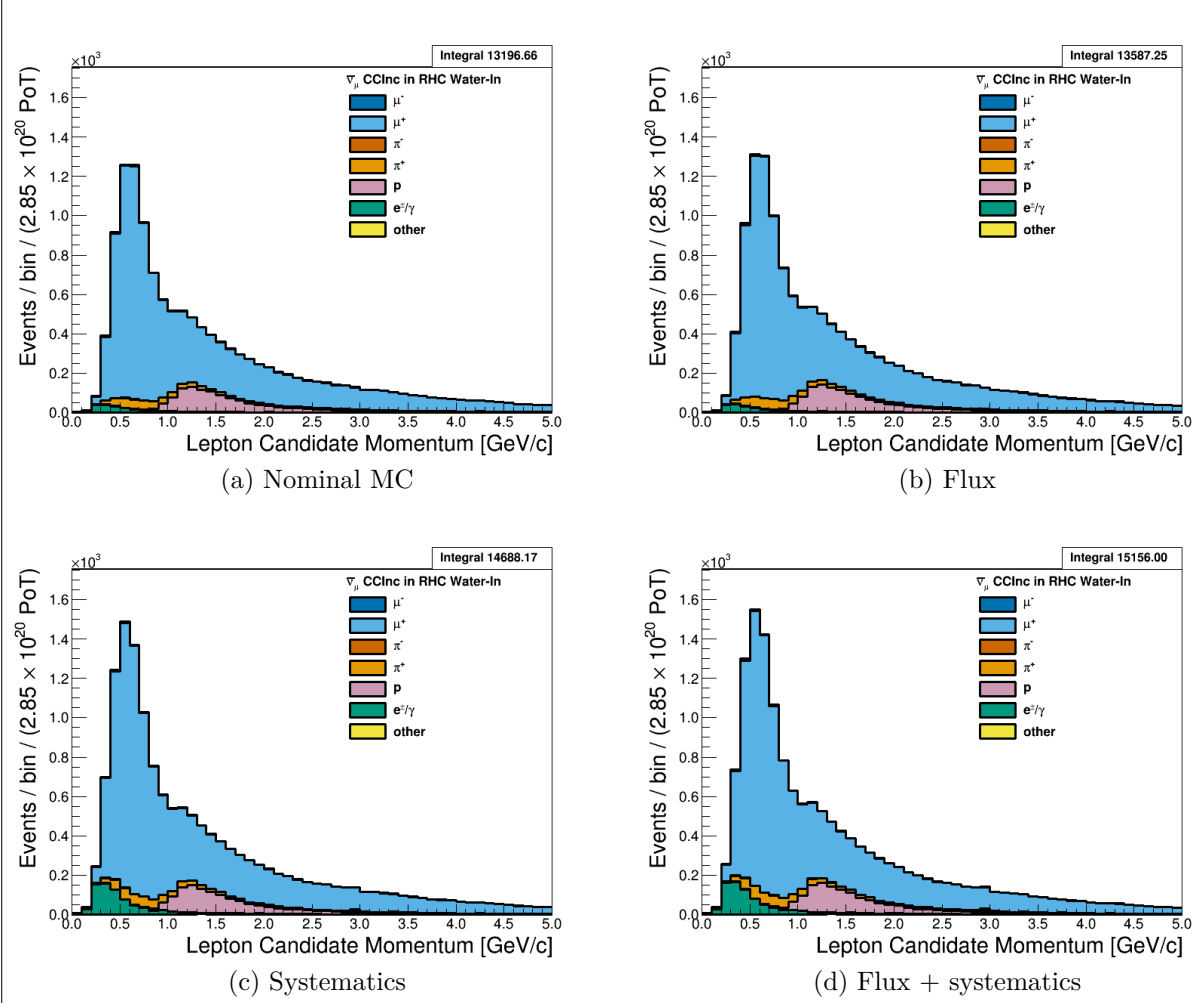


Figure 3.22: Reconstructed lepton candidate momentum separated by true particle species for RHC $\bar{\nu}_\mu$ CC-Inc. events occurring in the PØD in water-out mode. (a) The nominal MC prediction without any weights applied. (b) The flux tuning is applied. (c) The systematic weighting is applied. (d) Both flux and systematic weighting is applied.

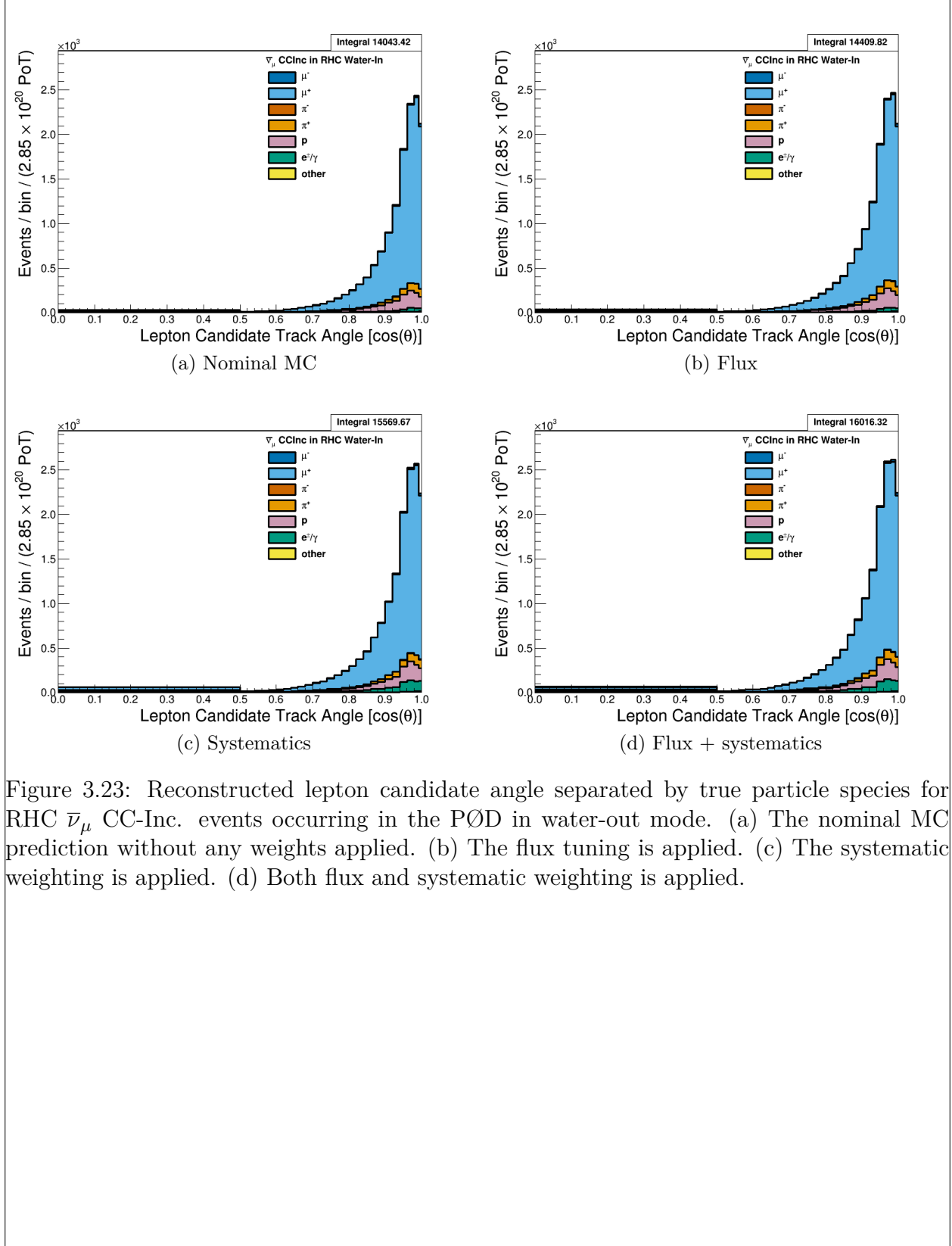


Figure 3.23: Reconstructed lepton candidate angle separated by true particle species for RHC $\bar{\nu}_\mu$ CC-Inc. events occurring in the PØD in water-out mode. (a) The nominal MC prediction without any weights applied. (b) The flux tuning is applied. (c) The systematic weighting is applied. (d) Both flux and systematic weighting is applied.

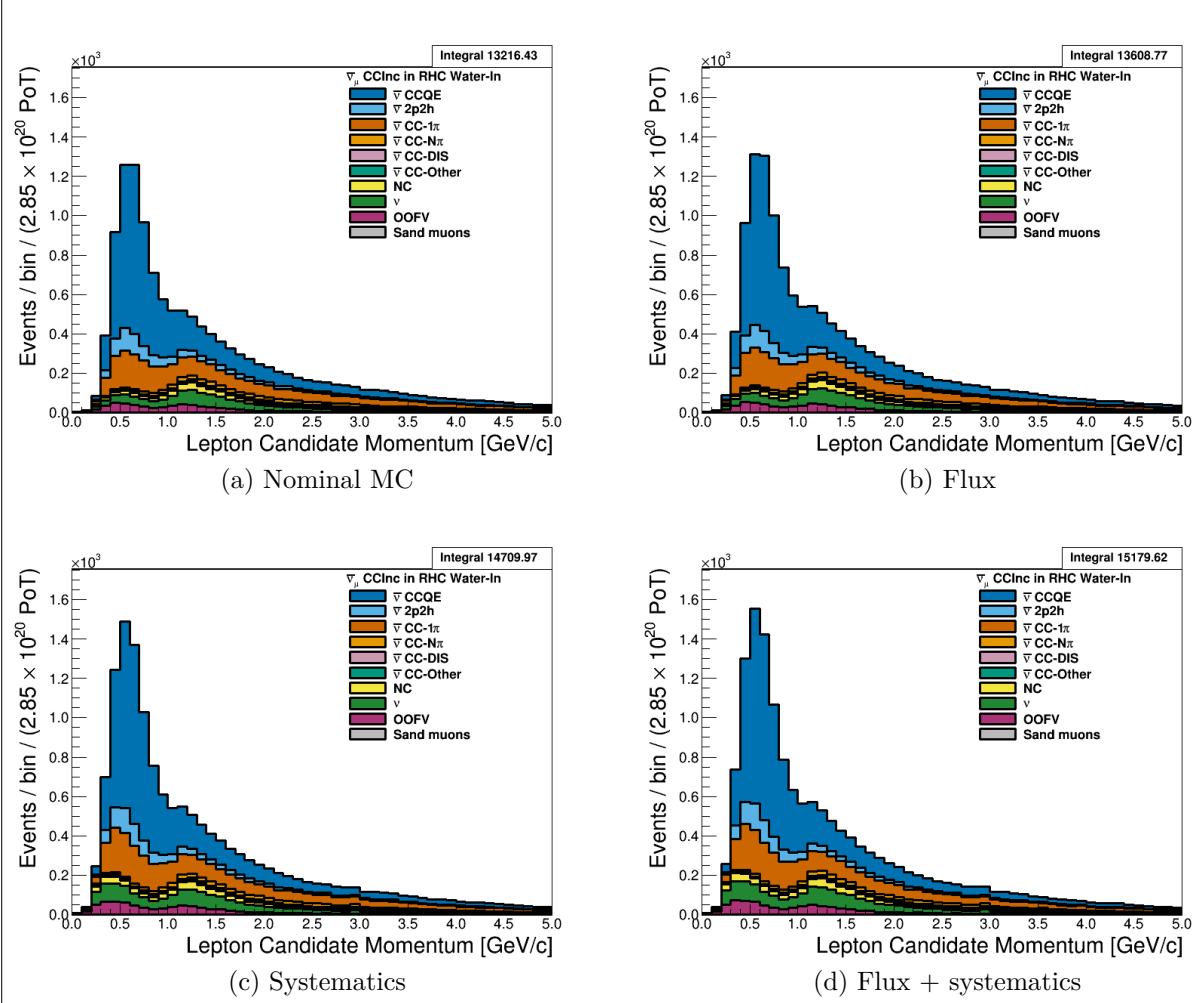


Figure 3.24: Reconstructed lepton candidate momentum separated by NEUT model interaction mode for RHC $\bar{\nu}_\mu$ CC-Inc. events occurring in the PØD in water-out mode. (a) The nominal MC prediction without any weights applied. (b) The flux tuning is applied. (c) The systematic weighting is applied. (d) Both flux and systematic weighting is applied.

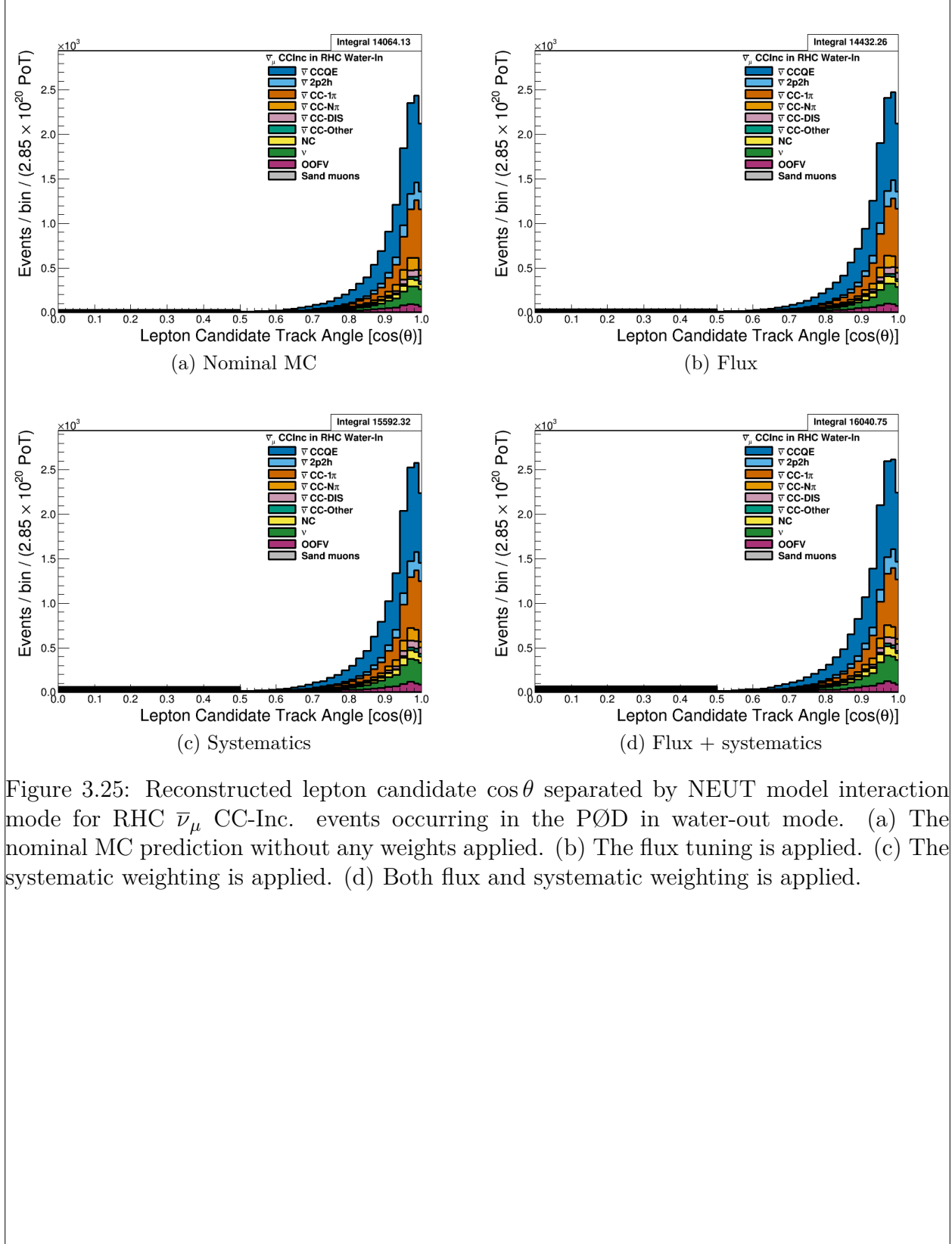


Figure 3.25: Reconstructed lepton candidate $\cos\theta$ separated by NEUT model interaction mode for RHC $\bar{\nu}_\mu$ CC-Inc. events occurring in the PØD in water-out mode. (a) The nominal MC prediction without any weights applied. (b) The flux tuning is applied. (c) The systematic weighting is applied. (d) Both flux and systematic weighting is applied.

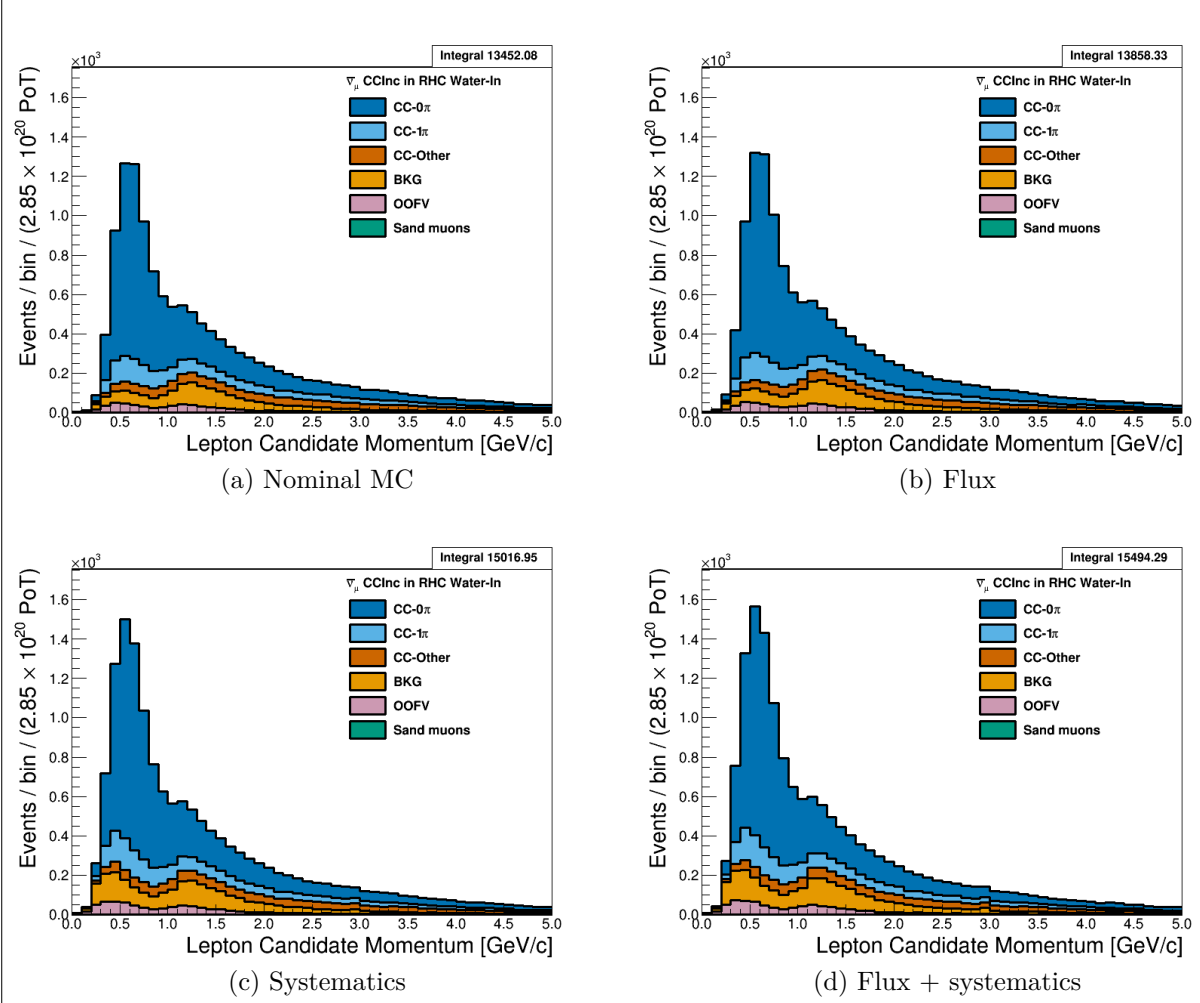


Figure 3.26: Reconstructed lepton candidate momentum separated by topology for RHC $\bar{\nu}_\mu$ CC-Inc. events occurring in the PØD in water-out mode. (a) The nominal MC prediction without any weights applied. (b) The flux tuning is applied. (c) The systematic weighting is applied. (d) Both flux and systematic weighting is applied.

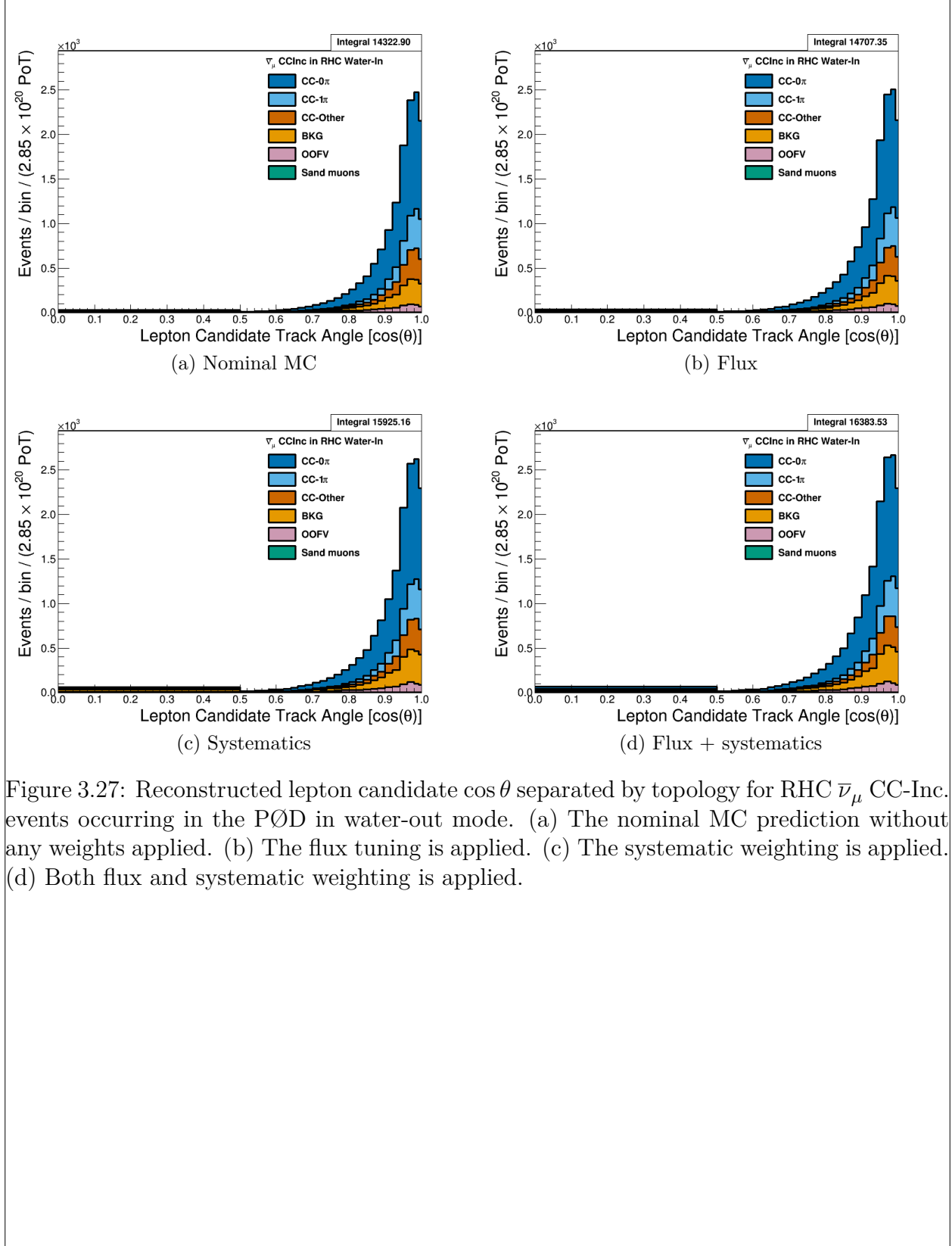


Figure 3.27: Reconstructed lepton candidate $\cos\theta$ separated by topology for RHC $\bar{\nu}_\mu$ CC-Inc. events occurring in the PØD in water-out mode. (a) The nominal MC prediction without any weights applied. (b) The flux tuning is applied. (c) The systematic weighting is applied. (d) Both flux and systematic weighting is applied.

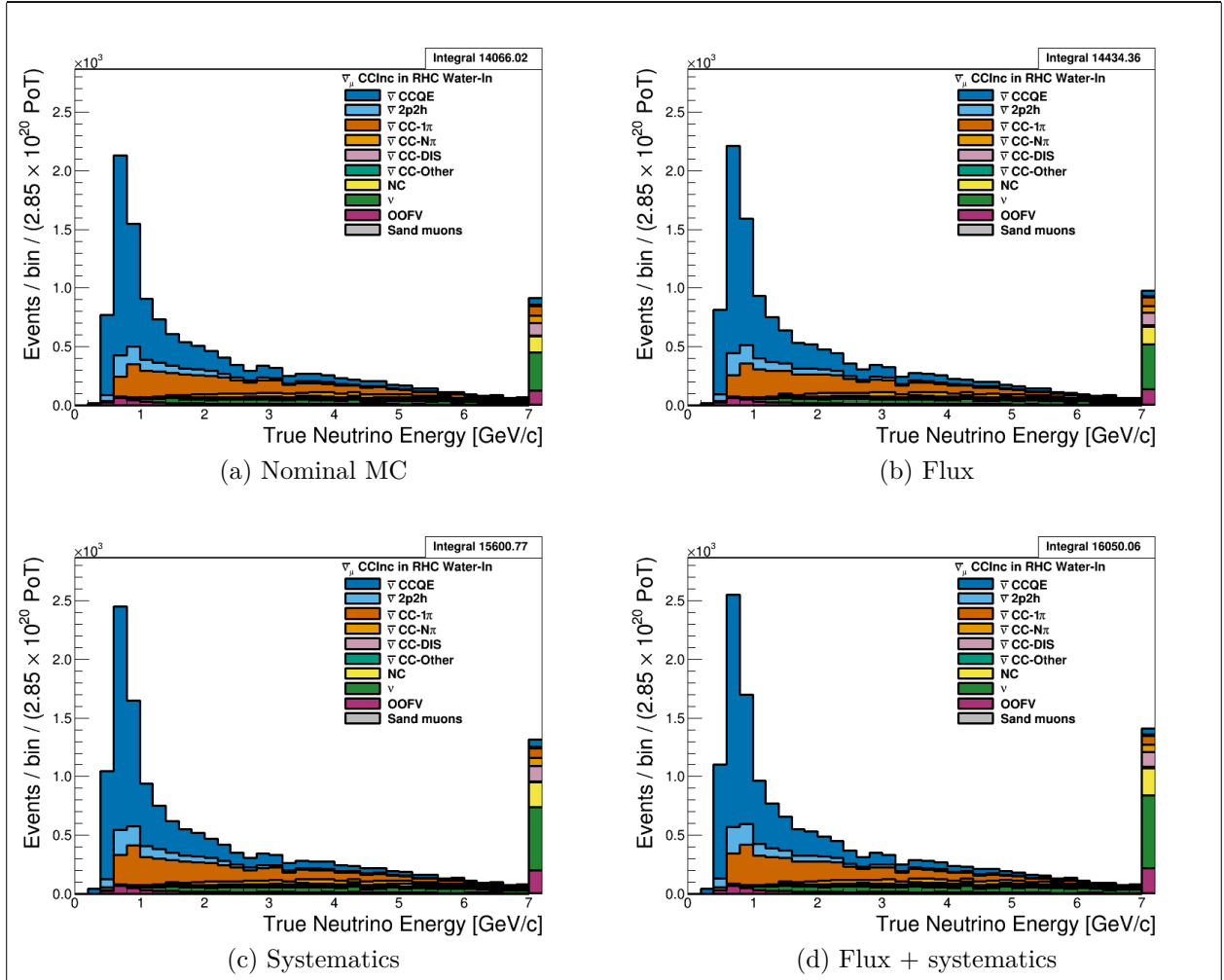


Figure 3.28: True neutrino energy associated with the lepton candidate separated by NEUT model interaction mode for RHC $\bar{\nu}_\mu$ CC-Inc. events occurring in the PØD in water-out mode. (a) The nominal MC prediction without any weights applied. (b) The flux tuning is applied. (c) The systematic weighting is applied. (d) Both flux and systematic weighting is applied.

ν_μ RHC: Add figures here

3.5.2 CC-1 Track (CCQE Enhanced)

Add figures here

3.5.3 CC-N Tracks (CCnQE Enhanced)

Add figures here

3.5.4 Differences Between Water-Out and Water-In Samples

327

4 **PØD-Only BANFF Parameterization**

328

PØD-only BANFF

5 Fitter Validation

Fitter validation

331 **6 Fitter Results**

332 Fitter results

7 Discussion

Discussion

References

- [1] S. Bienstock and Others. *Constraining the Flux and Cross Section Models with Data from the ND280 Detector using FGD1 and FGD2 for the 2017 Joint Oscillation Analysis*, August 2017. T2K-TN-324 v3. 13
- [2] S. Bolognesi and Others. *NIWG model and uncertainties for 2017 oscillation analysis*, April 2017. T2K-TN-315 v5. 13
- [3] T. Campbell. *Measurement of the ν_μ CC- 0π Double Differential Cross Section on Water in the PØD*, February 2018. T2K-TN-328. 16
- [4] T. Campbell and Others. *Analysis of ν_μ Charged Current Inclusive Events in the PØD in Runs 1+2+3+4*, Mar 2014. T2K-TN-80 v4. 16, 18, 19
- [5] R. Das and Others. *Measurement of Induced Charged Current Cross Section on Water using the PØD and TPC*, November 2014. T2K-TN-100. 16
- [6] K. Gilje. *Geometry and Mass of the π^0 Detector in the ND280 Basket*, Apr 2012. T2K-TN-73 v3.1. 19
- [7] M. Hartz and Others. *Constraining the Flux and Cross Section Models with Data from the ND280 Detector for the 2014/15 Oscillation Analysis*, May 2015. T2K-TN-220 v4. 8
- [8] A. Hillairet and Others. *ND280 Reconstruction*, Nov 2011. T2K-TN-72 v1. 19
- [9] G. Wikström and A. Finch. *Global Kalman vertexing in ND280*, Feb 2018. T2K-TN-46 v3. 17
- [10] T. Yuan and Others. *Double Differential Measurement of the Flux Averaged ν_μ CC0P Cross Section on Water*, Aug 2016. T2K-TN-258 v4.6.1. 16, 18

Nomenclature

CC-0 π A **charged current** zero pion selection is an exclusive selection that selects neutrino interaction topologies only one MIP-like particle.

CC-Inclusive A **charged current** event selection that selects all neutrino interaction topologies with an outgoing charged lepton.

FGD A **fine grain detector** is a detector made of closely spaced, small scintillating bars designed to provide precise resolution of charged particle tracks

FHC The **forward horn current** beam configuration that focuses positively charged particles into the particle decay pipe. This configuration produces a very pure ν_μ neutrino beam

HMNT The **highest momentum negatively-charged track** in the bunch

HMPT The **highest momentum positively-charged track** in the bunch

MIP A **minimum ionizing particle**

ND280 The **Near Detector** of T2K which is **280** meters away from the neutrino source.

CECal The **Central ECal** detector which is a part of the PØD inside ND280

PØD The π^0 detector (**pi-Ø detector**)

PØDule A collection of two active scintillator bar layers inside the PØD

RHC The **reverse horn current** beam configuration that focuses negatively charged particles into the particle decay pipe. This configuration produces a $\bar{\nu}_\mu$ enriched neutrino beam with a significant ν_μ contribution.

FV The **fiducial volume** of a detector is the region where the detector response is well understood

378 TPC A **t**ime **p**rojection **c**hamber is a device that detects and tracks charged particles with
379 the application of strong electric fields

380 Tracker The region of ND280 consisting of two FGDs and TPCs

381 Global The Global reconstruction module responsible for making joined tracks between the
382 subdetectors inside ND280

383 USECal The **U**pstream **E**Cal which is a part of the PØD inside ND280